

Robust Analog Lagrange Coded Computing: Theory and Algorithms via Discrete Fourier Transforms

Rimpi Borah and J. Harshan

Department of Electrical Engineering, Indian Institute of Technology Delhi, India

Abstract

Analog Lagrange Coded Computing (ALCC) is a recently proposed computational paradigm wherein certain computations over analog datasets are efficiently performed using distributed worker nodes through floating point representation. While the vanilla version of ALCC is known to preserve the privacy of the datasets from the workers and also achieve resilience against stragglers, it is not robust against Byzantine workers that return erroneous results. Highlighting this vulnerability, we propose a secure ALCC framework that is resilient against a wide range of integrity threats from the Byzantine workers. As a foundational step, we use error-correction algorithms for Discrete Fourier Transform (DFT) codes to build novel reconstruction strategies for ALCC thereby improving its computational accuracy in the presence of a bounded number of Byzantine workers. Furthermore, capitalizing on some theoretical results on the performance of the DFT decoders, we propose novel strategies for distributing the ALCC computational tasks to the workers, and show that such methods significantly improve the accuracy when the workers' trust profiles are available at the master server. Finally, we study the robustness of the proposed framework against colluding attacks, and show that interesting attack strategies can be executed by exploiting the inherent precision noise owing to floating point implementation.

Index Terms

Coded computing, Byzantine workers, Discrete Fourier transform codes, Colluding attacks, Precision noise.

I. INTRODUCTION

With the proliferation of data-centric methods for prediction, classification and other analytics, computation over the underlying large-scale dataset necessitates the use of distributed computing [1]. While such a framework reaps significant benefits when implemented over a set of trusted servers, it may pose significant challenges when applied over a network with a few untrusted servers. The notion of untrusted servers typically arises either in peer-to-peer networking, or when the underlying networks have

This work was presented in part at the IEEE International Symposium on Information Theory (IEEE ISIT 2024), held at Greece, July 2024 [28].

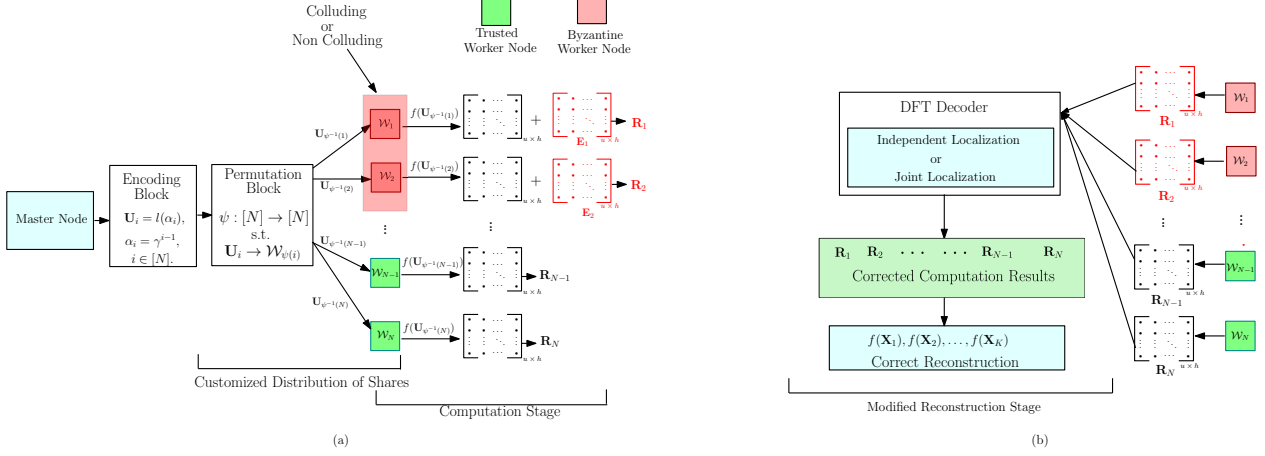


Fig. 1: Secure ALCC framework involving Byzantine worker nodes: (a) captures the phases of encoding at the master sever and distributed computation at the workers where Byzantine workers inject noise into their computations. (b) depicts the reconstruction stage at the master server wherein DFT decoders are used to nullify the noise introduced by the Byzantine workers.

poor security features. In such scenarios, distributed computing is vulnerable to (i) privacy issues on the dataset, (ii) distributed denial-of-service (DDoS) attacks, which could stall the overall compute operation, and (iii) integrity attacks, which leads to poor accuracy in the end result [2], [3]. Although there exists a number of cryptographic approaches to handle privacy, DoS and integrity attacks [4], those methods are not feasible for distributed computing owing to high computational loads, and moreover, those methods are not information-theoretically secure as the hardness assumption is based on computational boundedness.

As a promising alternative to the multi-layered cryptographic architecture, distributed coded computing architectures have been studied, in which tools from secret sharing schemes and coding-theory have been used to facilitate secure computations in the presence of aforementioned attacks. In particular, such coded computing architectures are known to provide efficient computation in the presence of the so-called *stragglers* [5]–[7], *Byzantine* workers [6]–[13], and *honest-but-curious* workers [7], [9], [13]–[16]. One notable example of such a coded computing paradigm is Lagrange Coded Computing (LCC) [17], which is a distributed coded computation framework that provides all the aforementioned features, when the function of interest is an arbitrary multivariate polynomial. Despite these benefits, the major limitation of LCC framework lies in its reliance on finite field dataset. As a result, its computation accuracy significantly suffers due to performance degradation because of overflows arising from finite field operations, especially when dealing with large datasets. To address this accuracy issue of LCC, Analog Lagrange Coded Computing (ALCC) has been proposed [18], wherein computations are directly performed over analog datasets using distributed worker nodes through floating point implementation. Notably, the accuracy of ALCC remains constant regardless the size of the datasets, and therefore, it outperforms LCC.

A. Motivation

Despite the scalability benefits offered by ALCC [18], we highlight that it does not provide all the security features offered by LCC. Specifically, while ALCC is known to provide resiliency against stragglers [18] and preserve the privacy of dataset from the honest-but-curious workers [15], [16], it is not resilient against Byzantine workers that return erroneous computation results. In this context, Byzantine workers refer to those worker nodes in the distributed setup that intentionally return erroneous computations to the master server, thereby degrading the overall accuracy of ALCC. Identifying this limitation, the authors of [18] make the following remarks in their conclusions: “*Another direction is to extend ALCC in order to take into account the presence of Byzantine workers, i.e., the worker nodes that deliberately send erroneous computation results*”. To the best of our knowledge, this direction has not been addressed hitherto in a comprehensive manner. Towards bridging this research gap, we investigate the security vulnerabilities of ALCC in the presence of Byzantine worker nodes, and ask a wide range of questions towards building a robust ALCC framework. Specifically, we ask the following questions: (i) Since the ALCC operations are over datasets with floating point representation, can we use coding-theoretic methods at the master server to detect and correct the errors added by the Byzantine workers directly using floating point data? (ii) ALCC typically involves encoding operation of the datasets at the master server, followed by distribution of computation tasks to the worker nodes, and finally the reconstruction stage at the master where the computed results from the workers are combined to get the desired end result. In scenarios where the master server has access to the trust profiles of the workers, can we redesign the encoding and distribution phases of ALCC to improve its accuracy in the presence of Byzantine workers? (iii) Once a robust ALCC framework is designed, based on Kerckhoffs’s principle [19] in cryptography, it is typical to expect the Byzantine worker nodes to have the knowledge of the reconstruction mechanism employed at the master node. Under such scenarios, can the floating point operations in ALCC be exploited by the Byzantine worker nodes to design novel colluding attacks?

B. Contributions

Although erroneous computations at a Byzantine worker node could be due to non-adversarial events such as bugs in software, in this work, we assume that Byzantine nodes are those nodes that have been compromised by external adversarial agents due to poor security features [20]. To capture a generic ALCC setting, unlike [18], we assume that the trust profiles of the workers are classified into two groups, namely: i) *reliable* worker nodes, those who are extremely trustworthy and never corrupt their computations, and ii) *unreliable* worker nodes, referred to those that may corrupt their computations at any point of time. Our

specific contributions, which are applicable for ALCC with arbitrary number of reliable and unreliable worker nodes, are listed below:

1) Our preliminary investigation reveals that the ALCC framework suffers from poor accuracy in the presence of Byzantine worker nodes (see Section II-D). Towards fixing this issue, we identify that in the absence of Byzantine worker nodes, the computations returned by the worker nodes in ALCC framework are essentially a set of codewords of a Discrete Fourier Transform (DFT) code [21]–[26] (see Section III). As a consequence, if Byzantine worker nodes return noisy computations, the introduced errors can be corrected by applying the error correction algorithms for the DFT code before the reconstruction stage of ALCC (see Section III). When using the DFT decoder at the master server, we show that ALCC suffers from degradation in accuracy due to the inaccurate localization of errors caused by precision noise from floating point operations. Identifying this dominance, we present bounds on the error rates in the recovery of the location of Byzantine worker nodes as a function of various ALCC parameters including the variance of the precision noise (see Section IV-A).

2) When employing the error correction algorithms of the DFT code, we discover that the algebraic structure of the computations returned by the worker nodes necessitates the master node to solve the roots of multiple error locator polynomials which may have a common set of solutions. Identifying this ALCC requirement, we use the bounds on the error rates of localization to propose a novel joint-localization algorithm for nullifying the erroneous computations returned by the Byzantine worker nodes, thereby enhancing the accuracy of ALCC. Through experimental results, we show that ALCC along with the proposed joint localization method provides significant accuracy benefits than that of [18] in the presence of Byzantine worker nodes (see Section IV-B).

SI	Salient features	LCC [17]	ALCC [18]	DFT decoders [21]–[26]	Our work
1	Straggler resilience	✓	✓	-	✓
2	Security against Byzantine workers	✓	✗	-	✓
3	Privacy against curious workers	✓	✓	-	✓
4	Analog domain support	✗	✓	-	✓
5	Error detection and correction capability	✓	✗	-	✓
6	Customized distribution of shares to workers	✗	✗	-	✓
7	Design of colluding attack strategies	✗	✗	-	✓
8	Bounds on the performance analysis of error localization of DFT decoder	-	-	✗	✓

TABLE I: Novelty of our work with respect to various features.

3) For the ALCC setting when the identities of the unreliable and reliable worker nodes are known to the master server, we derive bounds on the error rate of the localization block of the DFT decoder, and then use

them to design a customized strategy for distributing the encoded shares among unreliable worker nodes. Through experimental results, we show that our strategy serves as a low-complexity tractable method for parameter optimization, and provides significant benefits in accuracy of ALCC. We also show that our method performs close to other exhaustive-search based methods, which are impractical to implement in practice (see Section [V](#)).

4) With the support of derived theoretical bounds on the error rate of localization and its behavior with the variance of precision noise, we study the vulnerabilities of ALCC framework in the presence of *colluding* Byzantine worker nodes. In particular, we propose novel attack strategies from the perspective Byzantine workers, aiming at maximizing the error rate of localization, thereby degrading the accuracy of ALCC. These attack strategies are designed based on the sparsity of the noise matrices introduced by the Byzantine worker nodes and the communication overhead constraint imposed by the colluding channels among them. As the main takeaway, we prove a counter-intuitive result that not all the adversaries should inject noise in their computations in order to optimally degrade the accuracy of the ALCC framework. This is the first work of its kind to address the vulnerability of ALCC against colluding adversaries (see Section [VI](#)).

C. Novelty

As motivated in Section [I-A](#), our contributions are along the lines of LCC [\[17\]](#) and ALCC [\[18\]](#), wherein we have resolved some of the open problems in ALCC by providing resiliency against Byzantine worker nodes [\[6\]–\[13\]](#) under certain conditions. In particular, we have identified the utility of the DFT decoders [\[21\]–\[26\]](#) in ALCC, and have proposed novel encoding and decoding methods that are customized to ALCC. Some of the salient features offered by our work in comparison with the existing literature are tabulated in Table [I](#). To the best of our knowledge, this is the first work of its kind to present a coding-theoretic connection to ALCC. Although some preliminary results on this topic have been presented by our group in [\[27\], \[28\]](#), they do not provide analytical guarantees and proofs on the underlying ideas. While our work addresses robustness aspects of ALCC against Byzantine worker nodes, there also exists several contributions that focus on other aspects of coded computing such as numerical stability, privacy, straggler resilience, both with or without security features [\[29\]–\[38\]](#). However, we point out that none of them addresses the problem of securing ALCC, which was posed by the authors of [\[18\]](#).

II. ALCC WITH BYZANTINE WORKER NODES

The ALCC-based distributed computing setup, as illustrated in Fig. [1\(a\)](#) comprises a master node connected to N worker nodes, denoted by the set $\mathcal{W} = \{\mathcal{W}_1, \mathcal{W}_2, \dots, \mathcal{W}_N\}$, via dedicated links. Within this framework, the primary objective of the master node is to distribute a computational task $f(\cdot)$ on an

underlying dataset among the nodes in \mathcal{W} , and subsequently aggregate their computed results, leveraging their collective computing power. Further, we assume that \mathcal{W} is partitioned into two groups: i) *reliable* worker nodes, denoted by the set \mathcal{W}_{rel} , and ii) *unreliable* worker nodes, denoted by the set \mathcal{W}_{unrel} . Let τ and μ denote the number of reliable and unreliable worker nodes, respectively, such that $\tau + \mu = N$. In this context, reliable worker nodes are those that are proven to be honest and accurate in providing the intended computation results to the master node. In contrast, unreliable worker nodes are those that have not been proven honest, i.e., they may be curious about learning the dataset at the master node potentially compromising its privacy, and/or these nodes may return incorrect computation results to the master node. We assume that the master node knows \mathcal{W}_{rel} and \mathcal{W}_{unrel} .

For distributed computation, let $\mathbf{X} = (\mathbf{X}_1, \dots, \mathbf{X}_k)$ be the dataset held by the master node, where each $\mathbf{X}_j \in \mathbb{R}^{m \times n}$ for $j \in [k]$ such that $[k] \triangleq \{1, 2, \dots, k\}$. The master node aims to evaluate a polynomial $f : \mathbb{R}^{m \times n} \rightarrow \mathbb{R}^{u \times h}$ over the dataset \mathbf{X} . More specifically, the function $f(\cdot)$ is a D -degree polynomial wherein all the entries of the output matrix are multivariate polynomial functions of the entries of the input with a total degree not exceeding D . For instance, if $\mathbf{X}_j \in \mathbb{R}^{m \times n}$ is such that $x_{\bar{m}\bar{n}}$ is the (\bar{m}, \bar{n}) -th entry of \mathbf{X}_j , for $\bar{m} \in [m]$ and $\bar{n} \in [n]$, then $\mathbf{Y}_j = f(\mathbf{X}_j)$ refers to the output such that $y_{\bar{u}\bar{h}}$, which is the (\bar{u}, \bar{h}) -th entry of \mathbf{Y}_j , for $\bar{u} \in [u]$, $\bar{h} \in [h]$ is of the form $y_{\bar{u}\bar{h}} = f_{\bar{u}\bar{h}}(x_{11}, x_{12}, \dots, x_{mn})$, where $f_{\bar{u}\bar{h}}$ is a multivariate polynomial of degree D .

With the above dataset, the master node intends to compute $f(\cdot)$ in a decentralized fashion under the assumption that $f(\cdot)$ is known to all the workers nodes. Furthermore, similar to [18], the master node desires to execute distributed computation while ensuring resiliency against s number of straggler nodes in \mathcal{W} , and providing privacy from at most t curious worker nodes that intend to collude in order to learn the underlying dataset at the master node. In contrast to [18], along with the s stragglers and t curious worker nodes, in this work, we assume the presence of A Byzantine worker nodes who deliberately send erroneous computation results to the master node. Moreover, we assume that the set of A Byzantine worker nodes and the set of t curious worker nodes are subsets of \mathcal{W}_{unrel} . In contrast, s stragglers can be from \mathcal{W} irrespective of whether they are reliable or unreliable.

In the following subsections, we revisit ALCC, and apply it on our system model, which comprises straggler nodes, curious nodes and Byzantine worker nodes. To keep our focus on Byzantine worker nodes, we assume the absence of stragglers, i.e., $s = 0$, which implies that all the N worker nodes return their computation results to the master node.¹ We first outline the encoding strategy of vanilla ALCC followed by the computation and reconstruction stages for obtaining $\mathbf{Y}_j = f(\mathbf{X}_j)$, for $j \in [k]$. Although the encoding strategy is the same as that in [18], we modify the computation stage to take into account

¹For exposition, we have used $s = 0$, nonetheless, all the results of this work can be extended to the scenarios involving s stragglers.

the presence of Byzantine worker nodes.

A. Encoding in ALCC

To distribute the computational tasks among the workers, the master node creates $\mathbf{Z} = (\mathbf{X}_1, \mathbf{X}_2, \dots, \mathbf{X}_k, \mathbf{N}_1, \mathbf{N}_2, \dots, \mathbf{N}_t)$ where $\{\mathbf{N}_1, \mathbf{N}_2, \dots, \mathbf{N}_t\}$ are $m \times n$ random matrices with i.i.d. entries drawn from a zero-mean circular symmetric complex Gaussian distribution with standard deviation $\frac{\sigma}{\sqrt{t}}$. Here, the t random matrices are chosen to provide privacy on the dataset against a maximum of t curious worker nodes that may collude to recover the dataset. Let $\gamma = e^{-\frac{2\pi\iota}{N}}$ and $\omega = e^{-\frac{2\pi\iota}{k+t}}$ be the N -th and $(k+t)$ -th roots of unity, respectively, with $\iota^2 = -1$. With the above ingredients, Lagrange polynomial is used at the master node to construct the encoded dataset as

$$l(z) = \sum_{r=1}^k \mathbf{X}_r l_r(z) + \sum_{r=k+1}^{k+t} \mathbf{N}_{r-k} l_r(z), \quad (1)$$

where $l_r(\cdot)$'s are Lagrange monomials defined as

$$l_r(z) = \prod_{l \in [k+t] \setminus r} \frac{z - \beta_l}{\beta_r - \beta_l},$$

for all $r \in [k+t]$. Note that β_r 's are picked to be equally spaced on a circle of radius β centered around 0 in the complex plane such that $\beta_r = \beta\omega^{r-1}$ for $\beta \in \mathbb{R}^+$.

B. Distribution of Shares among the Worker Nodes

In this step, the master node evaluates $l(z)$ over the N -th roots of unity in the complex plane to obtain $\{\mathbf{U}_i = l(\alpha_i) \mid \alpha_i = \gamma^{i-1}, i \in [N]\}$. Further, to distribute the shares of the encoded dataset $l(z)$ among the worker nodes, we define a one-to-one mapping $\psi : [N] \rightarrow [N]$, such that the i -th evaluation \mathbf{U}_i goes to the worker node $\mathcal{W}_{\psi(i)}$, for $i \in [N]$. Although any of the $N!$ mappings can be used to distribute the shares, ALCC in [18] used the identity mapping where the i -th evaluation \mathbf{U}_i goes to the worker node \mathcal{W}_i .

C. Computation at the Workers

As per ALCC in [18], upon receiving \mathbf{U}_i from the master node, \mathcal{W}_i computes $f(\mathbf{U}_i) \in \mathbb{R}^{u \times h}$ and returns the result to the master node. However, with Byzantine worker nodes, we assume that some nodes return a corrupted version of their computations to the master node, as illustrated in Fig. 1(a). Formally, if i_1, i_2, \dots, i_A represent the indices of the Byzantine worker nodes, a worker node \mathcal{W}_{i_a} , is supposed to return $f(\mathbf{U}_{i_a})$. However, because of its adversarial nature, the corrupted version of $f(\mathbf{U}_{i_a})$

can be modelled as $f(\mathbf{U}_{i_a}) + \mathbf{E}_{i_a} \in \mathbb{R}^{u \times h}$ where, $\mathbf{E}_{i_a} \in \mathbb{R}^{u \times h}$ is the noise matrix chosen to corrupt the computation. Specifically, since all the computations are performed in floating-point representation, the computations received at the master node are

$$\mathbf{R}_i = f(\mathbf{U}_i) + \mathbf{E}_i + \mathbf{P}_i \in \mathbb{R}^{u \times h}, \quad (2)$$

where $\mathbf{E}_i = \mathbf{0}$ if $i \notin \{i_1, i_2, \dots, i_A\}$, and $\mathbf{E}_i \neq \mathbf{0}$ if $i \in \{i_1, i_2, \dots, i_A\}$, such that $\mathbf{P}_i \in \mathbb{R}^{u \times h}$ captures the precision errors due to the floating point operations at the worker nodes.

D. Function Reconstruction in ALCC

Ideally, in the absence of unreliable worker nodes and precision errors, i.e., when $\mathbf{E}_i = \mathbf{0}$ and $\mathbf{P}_i = \mathbf{0}$, upon receiving the set of computation results \mathbf{R}_i for $i \in [N]$ specified in (2) from N workers, the master node interpolates the polynomial $f(l(z))$ by using the results returned from at least $(k + t - 1)D + 1$ workers. Note that, $(k + t - 1)D + 1$ is the minimum number of returned evaluations needed to ensure a successful interpolation of $f(l(z))$ which results from the fact that the effective degree of $f(l(z))$ is $(k + t - 1)D$, where D indicate the degree of the target function $f(\cdot)$ and $k + t - 1$ represents the degree of the encoding polynomial $l(z)$ indicated in (1). Therefore, if \tilde{D} is used to represent $(k + t - 1)D$, indicating the effective degree of the polynomial $f(l(z))$, then the number of worker nodes required for successful interpolation of $f(l(z))$ is $K = \tilde{D} + 1$. Finally, to recover $f(\mathbf{X}_j)$'s, the master node computes $f(l(\beta_r))$ for $r \in [k]$. Note that these steps provide accurate reconstruction of $f(\mathbf{X}_j)$'s when $\mathbf{E}_i = \mathbf{0}$ and $\mathbf{P}_i = \mathbf{0}$. However, with precision noise and the noise added by the Byzantine workers, subsequent steps of evaluation and interpolation gets affected. Consequently, the recovered computation is noisy, degrading the overall accuracy.

To capture the above mentioned errors, let \mathbf{Y}' represent an estimate of $f(\mathbf{X})$ using ALCC. Similarly, let $\mathbf{Y} = f(\mathbf{X})$ represent the centralized computation performed locally at the master node without using ALCC. As a result, the relative error introduced by ALCC with respect to the centralized computation at the master node is computed as,

$$e_{rel} \triangleq \frac{\|\mathbf{Y} - \mathbf{Y}'\|}{\|\mathbf{Y}\|}, \quad (3)$$

where $\|\cdot\|$ denotes the l^2 -norm.

To demonstrate the impact of Byzantine worker nodes and precision errors on the accuracy of ALCC, we conduct experiments in the presence of Byzantine worker nodes to compute $f(\mathbf{X}) = \mathbf{X}^T \mathbf{X}$ such that $\mathbf{X} \in \mathbb{R}^{20 \times 5}$. The parameters used are $N = 31$, $k = 5$, $t = 3$, where $\tau = 0$ and computations from $K = 15$ worker nodes are used for reconstruction. Specifically, we compute the average relative error of ALCC

framework using (3) at different precision noise variances, while varying the number of Byzantine worker nodes. These results are presented in Fig. 2, which highlight that the relative error of ALCC increases significantly in the presence of Byzantine worker nodes, thereby confirming that the ALCC framework in [18] is not resilient against the presence of Byzantine workers.

Owing to this limitation, in the next section, we propose a robust ALCC framework that is resilient against the presence of Byzantine worker nodes under certain conditions.

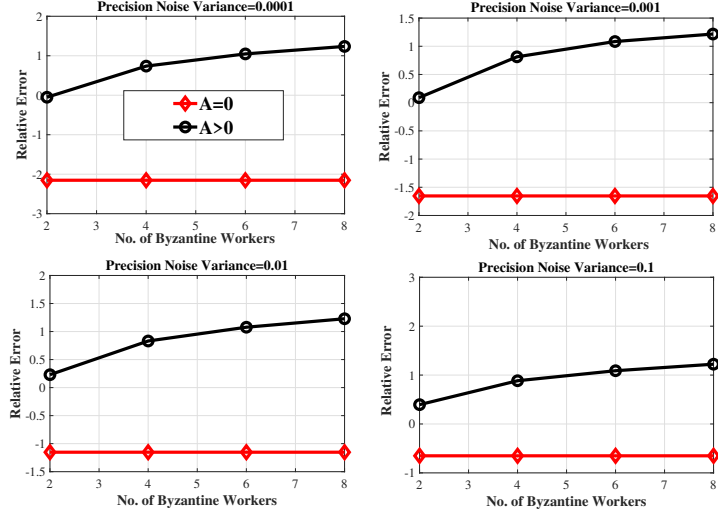


Fig. 2: Average relative error (in dB scale) of ALCC with parameters $N = 31, K = 15, \beta = 1.5, t = 3, \sigma = 10^6$. Here, the non-zero entries of noise matrices $\{\mathbf{E}_{i_a}\}$ introduced by the Byzantine worker nodes are i.i.d. as $\mathcal{CN}(10, 10^3)$.

III. SECURE ALCC FRAMEWORK

In this section, we consider a variant of ALCC wherein all the worker nodes are unreliable i.e., $\tau = 0$, such that $\mathcal{W} = \mathcal{W}_{unrel}$.² Furthermore, we assume the presence of A Byzantine worker nodes, where $0 < A < N$. Within this framework, we follow the same strategy for encoding the dataset and distributing its shares among the worker nodes as outlined in the previous section. However, in order to secure the framework against the Byzantine worker nodes, we propose a modification to the reconstruction stage. Recall the set of computation results returned by the worker nodes, denoted by, $\{\mathbf{R}_i \in \mathbb{R}^{u \times h} \mid i \in [N]\}$, where \mathbf{R}_i is specified in (2). Based on the structure of \mathbf{R}_i , the following proposition establishes the foundational result of this work.

Proposition 1. *For an ALCC setting with parameters N and $K = (k + t - 1)D + 1$, the erroneous computations returned by the A Byzantine worker nodes can be nullified as long as $A \leq v \triangleq \lfloor \frac{N-K}{2} \rfloor$ and the floating-point operations of ALCC have infinite precision.*

²The case of $\tau = 0$ has been considered only to introduce the proposed ideas. However, variant of ALCC with $\tau \neq 0$ will be addressed in Section V.

Proof: We refer the readers to the proof given in Appendix A. ■

For DFT codes, both coding-theoretic and subspace-based error-correction algorithms are well known [21], [22], [23], [24], [25]. In general, their implementation involves the following steps: (i) computing the syndrome vector, (ii) estimating the number of errors, (iii) identifying the location of errors, and (iv) estimating the error values. Consequently, in the presence of Byzantine worker nodes, these algorithms can be independently applied on each noisy DFT codeword $\mathbf{r}_{\bar{u}\bar{h}}$ to recover an estimate of $f(\mathbf{U}_i)$ for $i \in [N]$. Subsequently, the reconstruction method discussed in Section II-D can be used to recover $f(\mathbf{X}_j)$, for $j \in [k]$, as shown in Fig. 1(b). In the next subsection, we present the typical steps of the DFT decoder [21], [22], [23] when $\mathbf{P}_i = \mathbf{0}$ for $i \in [N]$.

A. DFT Based Error Correction Algorithm for ALCC

Given the set of $M = u \times h$ noisy codewords at the master node as captured by \mathbf{R}_{eff} , the first step is to compute the syndrome vector for each noisy codeword. Specifically, for $\mathbf{r}_{\bar{u}\bar{h}}$, the syndrome vector is computed as

$$\mathbf{s}_{\bar{u}\bar{h}} = \mathbf{r}_{\bar{u}\bar{h}} \mathbf{H}^\dagger = \mathbf{e}_{\bar{u}\bar{h}} \mathbf{H}^\dagger, \quad (4)$$

where $\mathbf{s}_{\bar{u}\bar{h}}$ represents a row vector of length $N - K$. Here, \dagger denotes the Hermitian operator, and \mathbf{H} denotes the parity check matrix of the (N, K) DFT code such that $\mathbf{G}\mathbf{H}^\dagger = \mathbf{0}$, where \mathbf{G} is the generator matrix. The vector $\mathbf{e}_{\bar{u}\bar{h}}$ represents the error vector of length N corresponding to the noisy codeword $\mathbf{r}_{\bar{u}\bar{h}}$ with Hamming weight A , where $\mathbf{e}_{\bar{u}\bar{h}} = [\mathbf{E}_1(\bar{u}, \bar{h}) \ \mathbf{E}_2(\bar{u}, \bar{h}) \ \dots \ \mathbf{E}_N(\bar{u}, \bar{h})]$. More specifically, the vector $\mathbf{e}_{\bar{u}\bar{h}}$ denotes the error values introduced by the A Byzantine worker nodes at the (\bar{u}, \bar{h}) entry of each noise matrix \mathbf{E}_i .

Using $\mathbf{s}_{\bar{u}\bar{h}}$ defined in (4), the next step is to estimate the number of errors introduced by the Byzantine worker nodes on each noisy codeword $\mathbf{r}_{\bar{u}\bar{h}}$. Note that, the noise injected by the Byzantine worker nodes into each entry of their respective noise matrices may be independent and vary in sparsity across different entries. As a result, the number of errors can differ across codewords, depending on the specific entries corrupted by the Byzantine worker nodes. Therefore, it is essential to estimate the number of errors for each noisy codeword $\mathbf{r}_{\bar{u}\bar{h}}$ individually before proceeding with error localization and correction. With infinite precision, the number of errors for a given noisy codeword $\mathbf{r}_{\bar{u}\bar{h}}$, can be estimated by finding the rank of the syndrome matrix \mathbf{S}_m , where the i -th row of the matrix \mathbf{S}_m is given by, $[\mathbf{s}_{\bar{u}\bar{h}}(1+i-1), \mathbf{s}_{\bar{u}\bar{h}}(2+i-1), \dots, \mathbf{s}_{\bar{u}\bar{h}}(v+i-1)]$ for $i = 1, 2, \dots, v$. Here, $v = \lfloor \frac{N-K}{2} \rfloor$, denotes the maximum error correction capability of the code, and $\mathbf{s}_{\bar{u}\bar{h}}(i)$ represents the i -th element of the syndrome vector $\mathbf{s}_{\bar{u}\bar{h}}$ corresponding to the noisy codeword $\mathbf{r}_{\bar{u}\bar{h}}$.

After estimating the number of errors introduced by the Byzantine worker nodes, denoted by $A_{\bar{u}\bar{h}}$, on the noisy codeword $\mathbf{r}_{\bar{u}\bar{h}}$, the next step is to compute the error locator polynomial $g_{\bar{u}\bar{h}}(z)$, which has degree $A_{\bar{u}\bar{h}}$, corresponding to the noisy codeword $\bar{\mathbf{r}}_{\bar{u}\bar{h}}$. The coefficients of the error locator polynomial $g_{\bar{u}\bar{h}}(z)$ are computed by solving the following system of linear equations,

$$\mathbf{s}_{\bar{u}\bar{h}}(i)g_{A_{\bar{u}\bar{h}}} + \mathbf{s}_{\bar{u}\bar{h}}(i+1)g_{A_{\bar{u}\bar{h}-1}} + \dots + \mathbf{s}_{\bar{u}\bar{h}}(i+A_{\bar{u}\bar{h}}-1)g_0 = -\mathbf{s}_{\bar{u}\bar{h}}(i+A_{\bar{u}\bar{h}}), \quad (5)$$

for $i = 1, 2, 3, \dots, 2v - A_{\bar{u}\bar{h}}$, where $g_0, g_1, \dots, g_{A_{\bar{u}\bar{h}}}$, and $g_0 = 1$ represents the coefficients of the error locator polynomial $g_{\bar{u}\bar{h}}(z)$. Further, the roots of error locator polynomial $g_{\bar{u}\bar{h}}(z)$ indicate the location of the errors.

After identifying the location of the errors, the next step is to compute the error vector $\mathbf{e}_{\bar{u}\bar{h}}$ for each noisy codeword $\mathbf{r}_{\bar{u}\bar{h}}$ by solving the system of linear equations specified in (4). Once the error vector for a noisy codeword is determined, these values are subtracted from its corresponding error locations to correct those errors. The corrected codewords are then used for the subsequent reconstruction stage.

All the internal blocks of DFT decoder discussed above assume $\mathbf{P}_i = \mathbf{0}$ on each \mathbf{R}_i for $i \in [N]$. However, in practice, the decoder suffers from performance degradation due to inherent precision noise introduced by the worker nodes when computing $f(\mathbf{U}_i)$, arising from floating point operations. As a result, $\mathbf{P}_i \neq \mathbf{0}$ for each \mathbf{R}_i , $i \in [N]$. To address this, several variations of the above mentioned steps of DFT decoder are available in the literature [21]–[26], and those can be adopted to operate under such finite-precision scenarios. Although, all the blocks of the DFT decoder are affected by finite-precision errors, the most vulnerable block is the error localization block. This is because the inherent precision noise perturbs each coefficient of the error locator polynomial which may lead to incorrect identification of error locations. As a consequence, accurately determining the roots in the presence of precision noise is a challenging task.

In the next section, we first analyze the performance of the error localization block of the DFT decoder, and then use its behavior to propose new methods of error localization.

IV. ERROR LOCALIZATION FOR SECURE ALCC

Recall that the master node retrieves $M = u \times h$ noisy DFT codewords $\{\mathbf{r}_{\bar{u}\bar{h}}\}$, each perturbed by precision noise. In this context, we apply a variant of the error correction algorithm discussed in the previous section on each noisy codeword, and present the performance of the error localization block.

A. Independent Error Localization in ALCC

In order to localize the errors introduced by the Byzantine worker nodes, we apply DFT decoder on each noisy codeword $\mathbf{r}_{\bar{u}\bar{h}}$ independently, assuming the number of errors on the corresponding noisy codeword

$\mathbf{r}_{\bar{u}\bar{h}}$ has been accurately estimated as $A_{\bar{u}\bar{h}}$, where $A_{\bar{u}\bar{h}}$ is within the error correcting capability of the code. Since the DFT decoder is applied independently on each noisy codeword $\mathbf{r}_{\bar{u}\bar{h}}$, for the ease of notation, in the rest of the section, we will use \mathbf{r} in place of $\mathbf{r}_{\bar{u}\bar{h}}$, A in place of $A_{\bar{u}\bar{h}}$, \mathbf{e} in place of $\mathbf{e}_{\bar{u}\bar{h}}$, and $g(z)$ in place of $g_{\bar{u}\bar{h}}(z)$. With finite precision, the noisy version of the error locator polynomial $g(z)$ is given by, $\bar{g}(z) = g(z) + e(z)$, where $g(z)$ denotes the error-locator polynomial with infinite precision and $e(z)$ is the error polynomial due to precision errors. When the additive noise entries are fixed, let the coefficients of $e(z)$ be modelled as i.i.d. as $\mathcal{CN}(0, \sigma_p^2)$, where σ_p^2 denote the variance of the precision noise. With infinite precision, the roots of the error locator polynomial accurately provide the information on position of the errors. For example, if X_q is a root of the polynomial $g(z)$, where $X_q = \gamma^{q-1}$ and $\gamma = e^{-\frac{2\pi i}{N}}$, with $q \in [N]$, then the index q corresponds to the location of the error. However, with precision errors, one needs to evaluate $\|\bar{g}(X_q)\|^2$ for each $q \in [N]$ and arrange the evaluations in the ascending order as $\|\bar{g}(X_{\hat{i}_1})\|^2 \leq \|\bar{g}(X_{\hat{i}_2})\|^2 \leq \dots \leq \|\bar{g}(X_{\hat{i}_N})\|^2$, where $\{\hat{i}_1, \hat{i}_2, \dots, \hat{i}_N\}$ is the ordered set based on the evaluations. Subsequently, the A smallest evaluations and its corresponding set of indices $\hat{\mathcal{L}} = \{\hat{i}_1, \hat{i}_2, \dots, \hat{i}_A\}$ are treated as the detected error locations [22], [24]–[26]. Further, the detected error locations are used to subtract the error vectors from the noisy codewords, to recover an estimate of $f(\mathbf{U}_i)$. Finally, these estimates of $f(\mathbf{U}_i)$ are used for the reconstruction stage.

In the rest of this section, we present an analysis on the error localization block. When recovering the roots of $g(z)$ of degree A , let the true locations of the errors be $\mathcal{L} = \{i_1, i_2, \dots, i_A\}$, however, let the recovered roots of $\bar{g}(z)$ be $\hat{\mathcal{L}} = \{\hat{i}_1, \hat{i}_2, \dots, \hat{i}_A\}$. Conditioned on this information, the localization step is in error if $\hat{\mathcal{L}} \neq \mathcal{L}$. Therefore, for a given choice of the error vector \mathbf{e} on codeword \mathbf{r} , the error rate of localization due to precision noise is

$$P_{error} = \text{Prob}(\hat{\mathcal{L}} \neq \mathcal{L}) = \text{Prob}\left(\bigcup_{a=1}^A i_a \notin \hat{\mathcal{L}}\right). \quad (6)$$

Furthermore, for i_a to not appear in $\hat{\mathcal{L}}$, there should be another index $j_b \in \mathcal{V} \triangleq [N] \setminus \mathcal{L}$, where $b \in \{1, 2, \dots, N-A\}$, such that $\|\bar{g}(X_{j_b})\|^2 \leq \|\bar{g}(X_{i_a})\|^2$. Denoting $\mathcal{V} = \{j_1, j_2, \dots, j_{N-A}\}$, we rewrite (6) and bound it as

$$\text{Prob}\left(\bigcup_{b=1}^{N-A} j_b \in \hat{\mathcal{L}}\right) \leq \sum_{b=1}^{N-A} \text{Prob}\left(j_b \in \hat{\mathcal{L}}\right). \quad (7)$$

Further, if $j_b \in \hat{\mathcal{L}}$, this implies $\|\bar{g}(X_{j_b})\|^2 \leq \|\bar{g}(X_{i_a})\|^2$ for some $a \in [A]$. Therefore, (7) can be expressed as

$$\leq \sum_{b=1}^{N-A} \text{Prob}\left(\|\bar{g}(X_{j_b})\|^2 \leq \|\bar{g}(X_{i_1})\|^2 \cup \|\bar{g}(X_{j_b})\|^2 \leq \|\bar{g}(X_{i_2})\|^2 \cup \dots \cup \|\bar{g}(X_{j_b})\|^2 \leq \|\bar{g}(X_{i_a})\|^2\right). \quad (8)$$

Applying union bound on (8), we obtain

$$P_{error} \leq \sum_{b=1}^{N-A} \sum_{a=1}^A \text{Prob}\left(\|\bar{g}(X_{j_b})\|^2 \leq \|\bar{g}(X_{i_a})\|^2\right), \quad (9)$$

$$= \sum_{b=1}^{N-A} \sum_{a=1}^A PEP_{j_b, i_a}, \quad (10)$$

where, PEP_{j_b, i_a} is given by

$$PEP_{j_b, i_a} = \text{Prob}\left(\|\bar{g}(X_{j_b})\|^2 \leq \|\bar{g}(X_{i_a})\|^2\right), \quad (11)$$

represents the pairwise error probability between i_a and j_b in (9). Therefore, in order to derive an expression for (10), we need to find an expression for the pairwise error probability between any two $A(N - A)$ pairs.

Since closed-form expressions on PEP_{j_b, i_a} are intractable to obtain, we propose a lower bound on it.

Theorem 1. *For a given A, N , σ_p^2 , and \mathbf{e} , a lower bound on the pairwise error probability in (11) can be expressed as*

$$PEP_{j_b, i_a} \geq PL_{j_b, i_a} \triangleq \frac{\kappa}{(1 + \kappa)} e^{-\frac{\eta(c_I^2 + c_Q^2)\kappa}{4\sigma_p^2(1 + \kappa)}}, \quad (12)$$

where η, c_I, c_Q are constants which depend on the vector \mathbf{e} and the indices j_b and i_a , and

$$\kappa = \frac{2}{\eta \sum_{l=1}^A 1 - \cos\left(l \frac{2\pi}{N} |j_b - i_a|\right)}.$$

Proof: We refer the readers to the proof given in Appendix B. ■

Based on the results in Theorem 1, we are now ready to make inferences on the behavior of the pairwise error probability as a function of σ_p^2 present the following corollary.

Corollary 1. *For a given A such that $A \leq \lfloor \frac{N-K}{2} \rfloor$, the lower bound in Theorem 1 is a non-decreasing function of σ_p^2 .*

The above statement implies that the lower bound on PEP_{j_b, i_a} is a non-decreasing function of σ_p^2 for all $j_b \in \mathcal{V}$ and $i_a \in \mathcal{L}$. Consequently, PEP_{j_b, i_a} is expected to degrade for non-negligible variance of precision errors for all $A(N - A)$ pairs. As a result, the overall upper bound on the error rate of localization in (9) increases with increasing σ_p^2 .

In order to showcase the effect of DFT decoder and to understand its behavior as a function of the precision noise variance σ_p^2 , we conduct experiments using (31, 15) DFT decoder in the ALCC setting to correct the errors introduced by the Byzantine worker nodes. The parameters and the function used for the

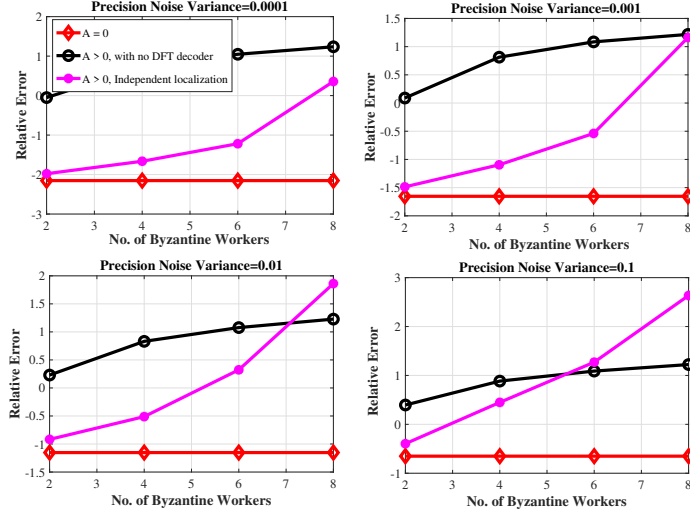


Fig. 3: Average relative error (in dB scale) of ALCC with parameters $N = 31, \tau = 0, K = 15, \beta = 1.5, t = 3, \sigma = 10^6$ with and without the DFT decoders in the presence of Byzantine worker nodes. Here, the non-zero entries of noise matrices $\{\mathbf{E}_{i_a}\}$ are i.i.d. as $\mathcal{CN}(10, 10^3)$.

experiments are same as that used to generate the results in Fig 2. Note that, for the above experiments, we assumed that the number of errors introduced by the Byzantine worker nodes in each noisy codeword is perfectly estimated at the decoder. Specifically, we compute the average relative error of ALCC when using the DFT decoder at different precision noise variance by varying the number of Byzantine worker nodes. These results are presented in Fig. 3. The plots in Fig. 3 confirm that ALCC framework with DFT decoder is robust to few Byzantine worker nodes present in the framework. However, when precision noise is high, as the number of Byzantine worker nodes increases the error localization performance degrades which validate the corollary 1. This degradation in accuracy renders the DFT decoder ineffective when used as an off-the-shelf block.

To address this limitation, in the next subsection, we show that the error-localization block of DFT decoder can be customized to improve the accuracy of ALCC.

B. ALCC Based Joint Error Localization

Recall that at the reconstruction phase of ALCC framework master node receives a total set of $M = u \times h$ codewords $\mathbf{r}_{\bar{u}\bar{h}}$ for $\bar{u} \in [u], \bar{h} \in [h]$. Consequently, when using DFT decoder in ALCC framework, at the input of the error-localization block a total of $M = u \times h$ error-locator polynomials corresponding to M noisy codewords $\{\mathbf{r}_{\bar{u}\bar{h}}\}$ are available along with their degree information which corresponds to the number of errors $A_{\bar{u}\bar{h}}$ introduced in $\mathbf{r}_{\bar{u}\bar{h}}$ by the Byzantine worker nodes. Since the sparsity of the set of noise matrices $\{\mathbf{E}_{i_a}\}$ for $a \in [A]$ injected by the Byzantine worker nodes can vary and unknown to the master node, the degree of the M error-locator polynomials can also vary accordingly.

Formally, for each \mathbf{E}_{i_a} , let $\mathbf{B}_{i_a} \in \{0, 1\}^{u \times h}$ specify the binary matrix that captures the positions of the non-zero entries of \mathbf{E}_{i_a} . These matrices are henceforth referred to as the *base matrices* for the Byzantine worker nodes. More specifically, a non-zero entry in a base matrix \mathbf{B}_{i_a} for $a \in [A]$ signifies that the corresponding component of the returned matrix $f(\mathbf{Y}_{i_a})$ is corrupted with an additive noise introduced by the worker node i_a . As a consequence, depending on the sparsity of the base matrices \mathbf{B}_{i_a} of the Byzantine worker nodes, the degrees of the M error locator polynomials vary. In general, when the degrees of the M error-locator polynomials are arbitrary, the master node can identify all the degree- v polynomials and average them component-wise to obtain a single polynomial. However, polynomials that have degree less than v cannot be averaged as their error locations are not guaranteed to be identical. Furthermore, since there are at most v Byzantine worker nodes, and all the polynomials should have a common subset of roots despite the presence of precision errors, the cardinality of the union of the roots of all the M polynomials should be bounded by v . Thus, conditioned on that, this highlights the need for jointly solving the roots of all the polynomials instead of solving for the roots of each polynomial independently.

Given the error-locator polynomials $\{\bar{g}_{\bar{u}\bar{h}}(z), \bar{u} \in [u], \bar{h} \in [h]\}$, let \mathcal{G}_v and \mathcal{G}_{v-} denote the set of polynomials with degree v and degree less than v , respectively. Then, we obtain a new set of polynomials, denoted by $\mathcal{G}_{joint} = \{\bar{g}_{max}\} \cup \mathcal{G}_{v-}$, where $\bar{g}_{max} = \frac{1}{|\mathcal{G}_v|} \sum_{\bar{g}_{\bar{u}\bar{h}}(z) \in \mathcal{G}_v} \bar{g}_{\bar{u}\bar{h}}(z)$ is the polynomial obtained by averaging the degree v polynomials. Furthermore, let $\bar{M} \leq M$ represent the cardinality of \mathcal{G}_{joint} . We now propose a method to jointly solve for the roots of \mathcal{G}_{joint} . Assuming that the polynomials of \mathcal{G}_{joint} are sorted in some order, let $t_m(x) \in \mathcal{G}_{joint}$ be the m -th polynomial of degree $d(m)$, where $1 \leq d(m) \leq v$. We propose to solve for the roots of every polynomial in \mathcal{G}_{joint} independently and then take the union of the roots. Let this set of roots be denoted by \mathcal{S}_I , which is of cardinality v'' . Furthermore, let $\mathcal{S}_{total} = \mathcal{S}_I^v$ be the set of all v -tuples over the set \mathcal{S}_I . For a given $\mathcal{S} \in \mathcal{S}_{total}$, we evaluate $t_m(z)$ at all the entries of \mathcal{S} , and obtain its first $d(m)$ smallest evaluations. Let the sum of the first $d(m)$ smallest evaluations of $t_m(z)$ be denoted by $E_{t_m(z)}(\mathcal{S})$, and the corresponding roots be $R_{t_m(z)}(\mathcal{S}) \subset \mathcal{S}$. Thus, the sum of the first $d(m)$ smallest evaluations of polynomials over the entire set \mathcal{G}_{joint} corresponding to \mathcal{S} is $\mathcal{E}_{\mathcal{S}} \triangleq \sum_{m=1}^{\bar{M}} E_{t_m(z)}(\mathcal{S})$. Also, the set of the roots of all the polynomials in \mathcal{G}_{joint} corresponding to \mathcal{S} is denoted by $\mathcal{R}_{\mathcal{S}} \triangleq \{R_{t_1(z)}(\mathcal{S}), R_{t_2(z)}(\mathcal{S}), \dots, R_{t_{\bar{M}}(z)}(\mathcal{S})\}$. Having obtained $\mathcal{E}_{\mathcal{S}}$ and $\mathcal{R}_{\mathcal{S}}$, we propose Problem 1.

Problem 1. For a given N , σ_p^2 , \mathcal{G}_{joint} , and v solve $\hat{\mathcal{S}} = \arg \min_{\mathcal{S} \in \mathcal{S}_{total}} \mathcal{E}_{\mathcal{S}}$, and then obtain $\mathcal{R}_{\hat{\mathcal{S}}}$ as its solution.

Note that as v'' (the cardinality of \mathcal{S}_I) increases, solving the optimization problem in Problem 1 becomes more computationally complex. However, in the practical scenario, when, σ_p^2 is small, the difference $v'' - v$

is expected to be small, which makes the optimization problem feasible to solve with computational complexity proportional to $\binom{v''}{v}$, even if $v'' \geq v$. In order to further decrease the complexity of solving the optimization problem, we substitute \mathcal{S}_I by \mathcal{S}_{II} , where \mathcal{S}_I is a randomly selected subset with the cardinality of \mathcal{S}_{II} is $v' \leq v''$ such that $\mathcal{S}_{II} \subseteq \mathcal{S}_I$. The parameter v' is referred to as the set constraint length for the proposed joint localization step, and this parameter can be adjusted to balance the computational complexity and error rate of joint localization. Therefore, increasing v' leads to improvement in accuracy, at the expense of higher computational complexity.

In a special case, when $\mathbf{B}_{i_a} = \mathbf{J}_{u \times h}$, where $\mathbf{J}_{u \times h}$ denotes the all-one matrix of size $u \times h$, this implies that every component of the returned matrix $f(\mathbf{Y}_{i_a})$ is corrupted with an additive noise by the worker node i_a . More specifically, when $\mathbf{B}_{i_a} = \mathbf{J}_{u \times h}$, it implies that all the error-locator polynomials have degree $v = \lfloor \frac{N-K}{2} \rfloor$. In this context, the following proposition demonstrates that the master node can localize the errors by evaluating the roots of only one error-locator polynomial. This polynomial is derived by taking the component-wise averaging of all the coefficients of M error locator polynomials.

Proposition 2. *When $\sigma_p^2 > 0$, if \mathbf{E}_{i_a} has non-zero entries in all its locations, for every $a \in [v]$, then joint localization can reduce its error rate compared to independent localization.*

Proof: We refer the readers to the proof given in Appendix C. ■

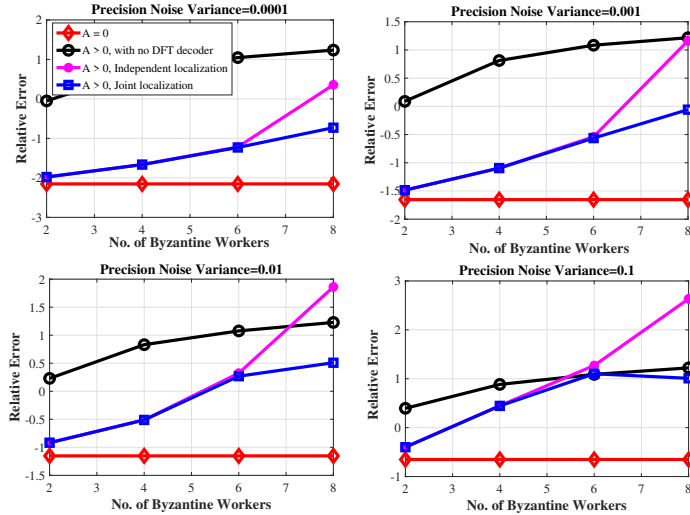


Fig. 4: Average relative error (in dB scale) of ALCC with parameters used for Fig. 3. For this plot, DFT decoders involving joint error localization are used in the presence of Byzantine worker nodes.

Corollary 2. *When M is large, and all the error-locator polynomials at the master node have degree v , the proposed joint localization significantly enhances the accuracy of root computation by effectively leveraging the redundancy across M error locator polynomials.*

The above statement implies that, when the set of M error-locator polynomials at the master node $\{\bar{g}_{\bar{u}\bar{h}}(z)\}$ have degree v and M is sufficiently large, we achieve a huge benefit on accuracy at the low computational complexity. More specifically, in this case, $\mathcal{G}_{joint} = \{\bar{g}_{max}\}$, where $\bar{g}_{max} = \frac{1}{|\mathcal{G}_v|} \sum_{\bar{g}_{\bar{u}\bar{h}}(z) \in |\mathcal{G}_v|} \bar{g}_{\bar{u}\bar{h}}(z)$ is the polynomial obtained by averaging the coefficients of M , degree v polynomials at the master node. Hence, we directly solve for the roots of the polynomial \mathcal{G}_{joint} , where the cardinality of the obtained sets of roots \mathcal{S}_I is contained to v , where $v \ll v''$. Furthermore, due to the averaging operation it substantially eliminates most of the precision noise present in the coefficients of M error locator polynomials, specifically when M is large, thereby providing better performance in error localization. In this context, we present a counter-intuitive claim that our proposed joint localization scheme outperforms better in terms of computational complexity and accuracy when A approaches v i.e., the error-correcting capability of the code.

To demonstrate the benefits of joint error localization over independent localization in terms of accuracy, we perform experiments in ALCC, when using (31, 15) DFT decoder at different precision noise variance σ_p^2 by varying the number of Byzantine worker nodes. The function and parameters used for the experiments are same as that used to generate the results in Fig 3. Note that, in order to generate the results we considered that the set of noise matrices $\{\mathbf{E}_{i_a}\}$ added by the Byzantine worker nodes are non zero i.e., $\mathbf{B}_{i_a} = \mathbf{J}_{u \times h}$, for $a \in [A]$. Furthermore, to generate the results on joint localization we use $\mathcal{S}_{total} = \mathcal{S}_I^v$. These results are presented in Fig. 4. From the plots shown in Fig. 4 we observe that, for the small precision noise variance σ_p^2 , the performance of independent localization and joint localization is similar. As we move towards the error-correcting capability of the code, the performance difference gradually increases and joint localization performs better in terms of accuracy. Further the plots in Fig. 4 confirm that joint localization outperforms independent localization especially when A is close to v .

Remark 1. We highlight that the error localization block of the DFT decoder enables a joint localization method to solve the roots of all the M error locator polynomials. This is because a common set of A Byzantine worker nodes inject noise on all the M DFT codewords in the ALCC setting. However, in the subsequent step of the DFT decoder where the error values are estimated, no such joint method is feasible across all the codewords. This is because the noise introduced by the Byzantine worker nodes on each codeword may not be identical, thereby leading to distinct syndrome vectors. Therefore, we suggest the master node to recover the error values from the noisy codewords in an independent manner.

V. SECURE ALCC WITH PROFILED WORKER NODES

In contrast to the ALCC setting discussed in Section III, in this section, we consider its variant comprising both reliable and unreliable worker nodes, i.e., $\tau > 0$ and $\mu > 0$, which implies \mathcal{W}_{unrel} is not a nullset. Furthermore, the case when $\tau \geq (\tilde{D} + 1)$ is irrelevant because $(\tilde{D} + 1)$ reliable worker nodes can

always be chosen for reconstruction. Therefore in this setup, the relevant range for τ is $0 < \tau < \tilde{D} + 1$. Within this framework, we use the same encoding strategy employed in the framework discussed in Section III, when $\tau = 0$. Further, while distributing the shares of the encoded data among the worker nodes any one-to-one mapping i.e., $\psi : [N] \rightarrow [N]$ can be used such that the i -th evaluation \mathbf{U}_i goes to the worker node $\mathcal{W}_{\psi(i)}$, for $i \in [N]$. However, in the subsequent discussion, we show that in the scenario where $0 < \tau < \tilde{D} + 1$, providing the identity mapping i.e., $\psi(i) = i$ may not be optimal in terms of relative error of the framework. In the reconstruction stage of ALCC, when using the DFT decoder with $\tau > 0$, we modify the block of error localization, particularly while computing the roots of the error locator polynomial $\bar{g}_{\bar{u}\bar{h}}(z)$. In this context, recall that the Byzantine worker nodes are a subset of the set of unreliable worker nodes. This implies that the evaluation of $\bar{g}_{\bar{u}\bar{h}}(z)$ should be restricted to those N -th roots of unity corresponding to the indices of unreliable worker nodes. Let the set of indices corresponding to μ unreliable worker nodes be $\mathcal{U} = \{i_{u_1}, i_{u_2}, \dots, i_{u_\mu}\}$, where $\mathcal{U} \subseteq [N]$ and $|\mathcal{U}| = \mu$, such that the indices of the Byzantine worker nodes $\mathcal{L} = \{i_1, i_2, \dots, i_A\} \subseteq \mathcal{U}$. Formally, in this variant of ALCC framework, with one-to-one mapping, we suggest evaluating $\bar{g}_{\bar{u}\bar{h}}$ at those N -th roots of unity corresponding to the indices present in the set \mathcal{U} instead of all N indices in the set $[N]$. More specifically, we evaluate $\|\bar{g}_{\bar{u}\bar{h}}(X_q)\|^2$, where $X_q = \gamma^{q-1}$ and $q \in \mathcal{U}$. We then arrange the evaluations in the ascending order in order to obtain

$$\|\bar{g}_{\bar{u}\bar{f}}(X_{\hat{i}_{u_1}})\|^2 \leq \|\bar{g}_{\bar{u}\bar{f}}(X_{\hat{i}_{u_2}})\|^2 \leq \dots \leq \|\bar{g}_{\bar{u}\bar{f}}(X_{\hat{i}_{u_\mu}})\|^2,$$

where $\{\hat{i}_{u_1}, \hat{i}_{u_2}, \dots, \hat{i}_{u_\mu}\}$ is the ordered set based on the evaluations. Subsequently, the A smallest evaluations and its corresponding set of indices $\hat{\mathcal{L}} = \{\hat{i}_{u_1}, \hat{i}_{u_2}, \dots, \hat{i}_{u_A}\}$ are treated as the detected error locations. Further, the following proposition captures the error rate of localization for ALCC with $\tau > 0$.

Proposition 3. *For an ALCC framework with N worker nodes, where $\mu > 0$, $0 < \tau < \tilde{D} + 1$, \mathcal{U} , and A Byzantine worker nodes with \mathcal{L} , an upper bound on error rate of localization can be expressed as*

$$\sum_{i=1}^{\mu-A} \sum_{a=1}^A \text{Prob} \left(\|\bar{g}_{\bar{u}\bar{f}}(X_{i_{u_i}})\|^2 \leq \|\bar{g}_{\bar{u}\bar{f}}(X_{i_a})\|^2 \right), \quad (13)$$

where $\mathcal{U} = \{i_{u_1}, i_{u_2}, \dots, i_{u_\mu}\}$, and $\mathcal{L} = \{i_1, i_2, \dots, i_A\}$.

Proof: This bound can be obtained along the similar lines of analysis in Section IV-A, except that the index of the erroneous detected location belongs to \mathcal{U} , instead of $[N] \setminus \mathcal{L}$. ■

Since the indices of Byzantine worker nodes are chosen randomly over \mathcal{U} , for a given $\mu > 0$, $0 < \tau < \tilde{D} + 1$ and A Byzantine worker nodes, an upper bound on average error rate of localization, denoted by $\bar{P}_{\text{error}} = \mathbb{E}_{\mathcal{L} \subseteq \mathcal{U}} [P_{\text{error}}]$, is

$$\mathbb{E}_{\mathcal{L} \subseteq \mathcal{U}} \left[\sum_{i=1}^{\mu-A} \sum_{a=1}^A \text{Prob} \left(\|\bar{g}_{\bar{u}\bar{f}}(X_{i_{u_i}})\|^2 \leq \|\bar{g}_{\bar{u}\bar{f}}(X_{i_a})\|^2 \right) \right]. \quad (14)$$

In the next section, we discuss the possibility of identifying a customized mapping $\psi(\cdot)$ in order to minimize the above average error rate of localization.

A. Assignment of Shares Based on Error Rate of Localization

Consider an ALCC setting where the unreliable worker nodes are such that \mathcal{U} consists of consecutive indices, such as $\{i, i+1, \dots, i+\mu-1\}$, for $i \in \{1, 2, \dots, N-\mu+1\}$, and the identity mapping is used for $\psi(\cdot)$ such that \mathbf{U}_i is assigned \mathcal{W}_i , for all $i \in [N]$. This implies that the unreliable worker nodes receive evaluations of the encoding polynomial $l(z)$ using the N -th roots of unity that are contiguous on the unit circle. As a result, this set of contiguous N -th roots of unity is used as candidate solutions when solving for the roots of the error locator polynomial $\bar{g}_{\bar{u}\bar{h}}(z)$ at the DFT decoder. Further, since the roots of $\bar{g}_{\bar{u}\bar{h}}(z)$ are computed by ordering its evaluations due to precision noise, an unreliable node, which is not a Byzantine worker node, may be wrongly detected as Byzantine due to its proximity to a true Byzantine node. Thus, using contiguous N -th roots of unity to the set of unreliable worker nodes may degrade the average error rate of localization. To address this problem, we believe that the subset of N -th roots of unity for assigning the evaluations to the unreliable workers must be carefully chosen at the master node. In this context, let $\mathcal{P} \subseteq [N]$ be the set of μ distinct indices used to pick the roots of unity for the evaluation of $l(z)$. Using this, we can construct the mapping $\psi(\cdot)$ such that for each index $j \in \mathcal{U}$, there exists a unique $i \in \mathcal{P}$ with $\psi(i) = j$. This ensures that, the unreliable worker node \mathcal{W}_j receives \mathbf{U}_i , where $i \in \mathcal{P}$. The remaining evaluations $\{\mathbf{U}_i : i \notin \mathcal{P}\}$ can be assigned to the reliable worker nodes \mathcal{W}_{rel} in an arbitrary manner. Note that the master node has a total $\binom{N}{\mu}$ ways of selecting the set \mathcal{P} . Therefore, to achieve a lower error rate of localization, one can choose the optimal set $\mathcal{P}^* \subseteq [N]$, which minimizes \bar{P}_{error} in (14). However, since there is no closed form expression for \bar{P}_{error} , in the rest of the section, we present a lower bound on it and use this as an objective function to formulate a minimization problem.

Note that any two pairs in the expression of \bar{P}_{error} in (14) can be lower bounded using Theorem 1. Therefore, instead of using \bar{P}_{error} as the objective function, its lower bound, which is obtained by applying the results of Theorem 1, can be used to formulate an optimization problem as

$$\arg \min_{\substack{\mathcal{P} \subseteq [N] \\ \text{s.t. } |\mathcal{P}|=\mu}} \left\{ \mathbb{E}_{\mathcal{L} \subseteq \mathcal{P}} \left[\sum_{i=1}^{\mu-A} \sum_{a=1}^A \frac{\kappa_{ia}}{(1+\kappa_{ia})} e^{-\frac{\eta H(\mathcal{L}, i) \kappa_{ia}}{4\sigma_p^2(1+\kappa_{ia})}} \right] \right\}, \quad (15)$$

where $\mathcal{P} = \{j_{u_1}, j_{u_2}, \dots, j_{u_\mu}\} \subseteq [N]$, denotes the set of evaluation indices for the unreliable worker nodes, and

$$\frac{\kappa_{ia}}{(1 + \kappa_{ia})} = \frac{2}{\eta \sum_{l=1}^A (1 - \cos(l \frac{2\pi}{N} |j_{u_i} - i_a|))}, \quad (16)$$

$$H(\mathcal{L}, i) = \left\| \prod_{a=1}^A (j_{u_i} - i_a) \right\|^2. \quad (17)$$

Here, $i_a \in \mathcal{L}$ for $a \in [A]$ denotes the evaluation indices for the Byzantine worker nodes, such that $\mathcal{L} \subseteq \mathcal{P}$. Given that the objective function in (15) is a tractable expression, the corresponding minimization problem can be solved through computational tools.

Further, we notice that instead of using $(\mu - A)A$ terms to compute the objective function, we can lower bound it again using the bound $\gamma_{min} \leq \frac{\kappa_{ia}}{(1 + \kappa_{ia})} \leq \gamma_{max}$, $\forall i, a$, to formulate the following optimization problem

$$\arg \min_{\substack{\mathcal{P} \subseteq [N] \\ \text{s.t. } |\mathcal{P}| = \mu}} \mathbb{E}_{\mathcal{L} \subseteq \mathcal{P}} \left[\sum_{i=1}^{\mu - A} \gamma_{min} e^{-\frac{\eta H(\mathcal{L}, i) \gamma_{max}}{4\sigma_p^2}} \right],$$

where γ_{min} and γ_{max} are constants, which can be computed offline. Although the above problem can be solved using numerical methods, we propose a variant of it in Problem 2, wherein the dominant term of the summation is used instead of the sum of the $\mu - A$ terms. Thus, for a given choice of $N, A, \mu > 0$, $0 < \tau < \tilde{D} + 1$, σ_p^2 , η , the master node in ALCC can obtain \mathcal{Q}^* by solving Problem 2, and then use it for assigning the shares among the unreliable worker nodes.

Problem 2. For ALCC with $\mu > 0$, $0 < \tau < \tilde{D} + 1$, and A Byzantine worker nodes, solve

$$\mathcal{Q}^* = \arg \min_{\substack{\mathcal{P} \subseteq [N] \\ \text{s.t. } |\mathcal{P}| = \mu}} \mathbb{E}_{\mathcal{L} \subseteq \mathcal{P}} \left[\max_{i \in \{1, 2, \dots, \mu - A\}} e^{-\frac{\eta H(\mathcal{L}, i) \gamma_{max}}{4\sigma_p^2}} \right].$$

B. Experimental Results

In order to showcase the effectiveness of our proposed method for assigning evaluation indices, we consider a baseline method wherein the set of evaluation indices for unreliable worker nodes is chosen by minimizing the average relative error of the ALCC framework. The solution to such a problem is denoted by \mathcal{R}^* . Note that this method is computationally infeasible as there is no closed form expression on relative error as a function of the system parameters, and therefore, experiments must be conducted to evaluate the relative error for each \mathcal{P} . Further, we conduct experiments within ALCC to obtain two sets of

evaluation indices for unreliable worker nodes, one using the baseline approach, and the other by solving Problem 2. Further, we compute the average relative error using the index sets from both methods, at their respective precision noise variances as presented in Table II. Additionally, we perform experiments when the evaluation indices assigned to the unreliable worker nodes are contiguous. Specifically, we compute the average relative error at different precision noise variances, while computing the function $f(\mathbf{X}) = \mathbf{X}^T \mathbf{X}$, such that $\mathbf{X} \in \mathbb{R}^{20 \times 5}$, using i) contiguous index sets, and ii) the index sets \mathcal{R}^* and \mathcal{Q}^* from Table II. Note that the average relative error is computed over 10^3 iterations, where the Byzantine worker nodes are chosen uniformly at random over the set of μ unreliable worker nodes in each iteration. The parameters used for the experiments are $N = 11, k = 3, t = 1, \beta = 1.5, \mu = 5, A = 2, K = 7, \eta = 10, \sigma = 10^6$. Here, the non-zero entries of noise matrices $\{\mathbf{E}_{i_a}\}$ are i.i.d. as $\mathcal{CN}(10, 10^3)$. These results are presented in Fig. 5. As illustrated in Fig. 5, assigning contiguous evaluation indices to the unreliable worker nodes leads to higher relative error compared to our proposed method of assigning the evaluation indices and the method that aims to minimize the average relative error of ALCC. Furthermore, the plots in Fig. 5 confirm that our proposed method of assigning evaluation indices to the unreliable worker nodes based on minimizing error rate of localization is not significantly away from the method that aims to minimize the average relative error, in terms of accuracy of the framework.

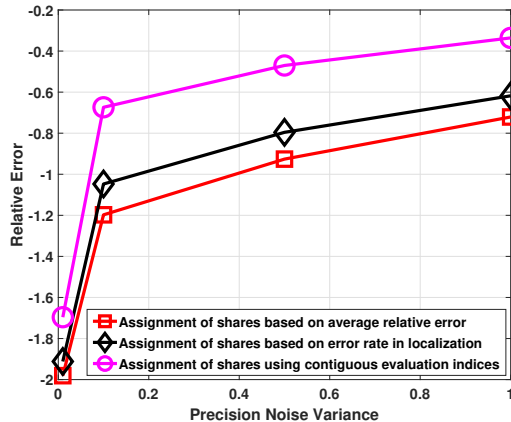


Fig. 5: Average relative error (in dB) when (i) indices are obtained by minimizing the average relative error of the framework, (ii) indices are obtained by solving Problem 2, and (iii) using contiguous indices.

Precision Noise Variance	\mathcal{R}^*	\mathcal{Q}^*
1	1, 2, 5, 8, 9	1, 3, 6, 9, 11
0.5	1, 4, 5, 8, 9	1, 3, 6, 9, 11
0.1	2, 5, 6, 9, 10	1, 3, 6, 8, 11
0.01	2, 4, 6, 8, 11	1, 2, 4, 5, 7

TABLE II: Evaluation indices for unreliable worker nodes obtained through minimizing the relative error of the framework and error rate of localization. Parameters used for the experiments are $N = 11, k = 3, t = 1, \beta = 1.5, \mu = 5, A = 2, K = 7, \eta = 10, \sigma = 10^6$.

When using ALCC with $\tau > 0$, note that the joint localization method in Section IV-B, can further reduce the error rate of localization compared to independent localization.

VI. SECURE ALCC WITH COLLUDING BYZANTINE WORKER NODES

In this section, we address some potential collusion attacks by the Byzantine worker nodes on ALCC. For exposition, we consider an ALCC setting comprising N worker nodes, where $\tau = 0$, such that $\mathcal{W} = \mathcal{W}_{unrel}$, implying that all the N worker nodes are unreliable.³ Therefore, we adopt the same encoding strategy, identity mapping for distributing the shares, and the same reconstruction strategy as discussed in Section III for the ALCC setting with $\tau = 0$. However, in contrast to the scenario discussed in Section III, in this setting we assume the presence of v Byzantine worker nodes, where $v = \lfloor \frac{N-K}{2} \rfloor$, denotes the error correcting capability of the DFT decoder. Further, we assume that the v Byzantine worker nodes have access to a dedicated colluding channel for communication.

Before proposing an optimized framework for colluding attacks, we look at a possible strategy through which the Byzantine worker nodes can inject noise matrices in order to maximize relative error of ALCC. Since there is no closed-form expression on relative error as a function of system parameters, we believe that the upper bound on the error rate of localization specified in (9) can be used as an objective function for maximization from the perspective of the Byzantine worker nodes. Although the nature of collusion is broadly applicable to decide the noise matrices $\mathbf{E}_{i_1}, \mathbf{E}_{i_2}, \dots, \mathbf{E}_{i_v}$, we focus primarily on a scenario where the Byzantine worker nodes collude to decide on the sparsity of their noise matrices. This is because, the sparsity of the noise matrices will decide the degree of the error locator polynomials, which in turn affects the error rate localization. Therefore, once the sparsity and the positions of the non-zero entries are chosen, we assume that non-zero entries are injected on those positions in a statistically independent manner.

Recall that for each \mathbf{E}_{i_a} , such that $a \in [v]$, $\mathbf{B}_{i_a} \in \{0, 1\}^{u \times h}$ specifies the binary matrix that captures the positions of the non-zero entries of each \mathbf{E}_{i_a} . Therefore, before formally addressing the problem on selecting the base matrices $\{\mathbf{B}_{i_1}, \mathbf{B}_{i_2}, \dots, \mathbf{B}_{i_v}\}$ in order to maximize the error rate of localization, Proposition 2 highlights an important consideration on how not to choose them. More specifically, from Proposition 2, if $\mathbf{B}_{i_a} = \mathbf{J}_{u \times h}$, $\forall a \in [v]$, then the master node receives a total of $M = u \times h$ polynomials of degree v which can be used to reduce the effective variance of precision noise across the coefficients of error locator polynomials, thereby minimizing the error rate of localization. Therefore, to counter this, Byzantine worker nodes must select their base matrices in order to forbid the master node from averaging the coefficients of the error locator polynomials. Therefore, to define a problem statement on

³However, these attacks are also applicable to scenarios when $\tau > 0$.

the choice of the base matrices $\{\mathbf{B}_{i_1}, \mathbf{B}_{i_2}, \dots, \mathbf{B}_{i_v}\}$, we first define the effective base matrix, denoted by $\mathbf{B}_{eff} \in \{0, 1\}^{uh \times v}$, as

$$\mathbf{B}_{eff} = \begin{bmatrix} \mathbf{B}_{i_1}(1, 1) & \mathbf{B}_{i_2}(1, 1) & \dots & \mathbf{B}_{i_v}(1, 1) \\ \mathbf{B}_{i_1}(1, 2) & \mathbf{B}_{i_2}(1, 2) & \dots & \mathbf{B}_{i_v}(1, 2) \\ \vdots & \vdots & \vdots & \vdots \\ \mathbf{B}_{i_1}(1, h) & \mathbf{B}_{i_2}(1, h) & \dots & \mathbf{B}_{i_v}(1, h) \\ \mathbf{B}_{i_1}(2, 1) & \mathbf{B}_{i_2}(2, 1) & \dots & \mathbf{B}_{i_v}(2, 1) \\ \vdots & \vdots & \vdots & \vdots \\ \mathbf{B}_{i_1}(u, h) & \mathbf{B}_{i_2}(u, h) & \dots & \mathbf{B}_{i_v}(u, h) \end{bmatrix}. \quad (18)$$

The above representation is such that the rows represent the M error locator polynomials, and the number of ones in a given row captures the degree of the corresponding error locator polynomial. Note that, for $1 \leq a \leq v$, the a -th column of \mathbf{B}_{eff} matrix corresponds to the entries of base matrices \mathbf{B}_{i_a} of a -th Byzantine worker which in turn implies that a -th column of \mathbf{B}_{eff} matrix is completely in control of the a -th Byzantine worker, but not the elements across the columns. As a result, the Byzantine worker nodes must collude in order to control the number of ones in a row, which in turn controls the degree of the error locator polynomials. Given that the master node has a total of M error locator polynomials captured by the rows of \mathbf{B}_{eff} , each of degree at most v , the relevant objective function from the perspective of Byzantine worker nodes is average error rate of localization across all M error locator polynomials. With this background, a problem for the Byzantine workers is to choose \mathbf{B}_{eff} , such that average error rate of the localization across M error locator polynomials is maximized. Based on this, we present Problem 3.

Problem 3. For a given σ_p^2 , N , M and v , solve

$$\mathbf{B}^*_{eff} = \arg \max_{\mathbf{B}_{eff} \in \{0, 1\}^{uh \times v}} \frac{1}{M} \left(\sum_{c=1}^M P_{error_c} \right) \quad (19)$$

wherein P_{error_c} denotes the error rate of localization for c -th error locator polynomial captured by c -th row of \mathbf{B}_{eff} , where $1 \leq c \leq M$.

Although the master node can either perform independent localization or joint localization in order to solve for the roots of M error locator polynomials, the combinatorial nature of Problem 1, makes it intractable to derive an exact expression on the error rate of joint localization for various set constraint lengths. To address this, we target an analytically-tractable variant of the joint localization step, and show that the Byzantine worker nodes can choose \mathbf{B}^*_{eff} , which maximizes the error rate of joint localization

method, wherein independent localization is performed on each polynomial in \mathcal{G}_{joint} , after averaging all the v degree polynomials.

Furthermore, the error rate of localization P_{error_c} for c -th error locator polynomial, appearing on the right hand side of the expression in (19) can be upper bounded using the expression specified in (9), where $c \in [M]$. Specifically, if the error locator polynomial corresponding to the c -th row of \mathbf{B}_{eff} has degree $A_c \leq v$, then the bound on the error rate in (9), involves a total of $A_c(N - A_c)$ pairwise error probabilities terms denoted by, $PEP_{j_b i_a}$ between each index $i_a \in \mathcal{L}$ and an index $j_b \in \mathcal{V}$. However, to simplify the bound analytically, we consider only the most dominant pairwise error term for each index $i_a \in \mathcal{L}$, i.e., the term with maximum $PEP_{j_b i_a}$ over all $j_b \in \mathcal{V}$, instead of accounting all $N - A_c$ terms in \mathcal{V} . More specifically, we consider the dominant event when j_b is the nearest neighbour of i_a , i.e., $j_b = i_a + 1$ modulo N or $j_b = i_a - 1$ modulo N . As a result, the upper bound on error rate of localization can be approximated as $2 \times \sum_{a=1}^{A_c} PEP_{dom}(i_a)$, where $PEP_{dom}(i_a)$ represents the pairwise error probability between the index i_a and its nearest neighbour. Also, the factor of 2 arises due to the symmetry in the N -th roots of unity. In this context, to keep our analysis tractable we consider the most dominant pair among these A_c distinct pairs. Hence, we approximate the upper bound on error rate of localization in (9) for c -th error locator polynomial of degree A_c as

$$P_{error_c} \leq A_c \times PEP_{dom}(i_a^*, c), \quad (20)$$

where $PEP_{dom}(i_a^*, c) = \max_{1 \leq a \leq A_c} PEP_{dom}(i_a)$, and $1 \leq c \leq M$. However, since the right-hand side of the error rate expression in (20) is not analytically tractable, we use the lower bound provided in Theorem 1 as a surrogate function for the pairwise error probability term $PEP_{dom}(i_a^*, c)$. Therefore, substituting the lower bound from Theorem 1 into (20), error rate of localization can be computed for each individual error locator polynomial of degree $A_c \leq v$ captured by the rows of \mathbf{B}_{eff} . Subsequently, the average error rate of localization across all M error locator polynomials can be obtained which serves as an analytically tractable objective function for solving the Problem 3. Hence, instead of solving Problem 3, we propose to solve Problem 4.

Problem 4. For a given σ_p^2 , N , M and v , solve

$$\mathbf{B}^{\dagger}_{eff} = \arg \max_{\{0,1\}^{u_h \times v}} \frac{1}{M} \left(\sum_{c=1}^M A_c \times PL_{(i_a^*, i_a^* + 1, c)} \right) \quad (21)$$

where $PL_{(i_a^*, i_a^* + 1, c)}$ denotes the lower bound on pairwise error probability between the dominant index i_a^* among A_c distinct terms and its nearest neighbour $i_a^* + 1$ for c -th error locator polynomial

captured by c -th row of \mathbf{B}_{eff} , where $1 \leq c \leq M$.

Given that the objective function of Problem 4 is available in closed-form, the Byzantine workers can obtain \mathbf{B}_{eff}^\dagger using numerical methods. However, to reduce the computational complexity, we believe that the following lemma can be used to directly identify the number of ones in a row of \mathbf{B}_{eff}^\dagger .

Lemma 1. *For a given N , when σ_p^2 is small, for an error locator polynomial of degree A_c , such that $A_c \leq v$, captured by a row of \mathbf{B}_{eff} , the expression $A_c \times PL_{(i_a^*, i_a^* + 1, c)}$ in (21) is a non-decreasing function of A_c .*

Proof: We refer the readers to the proof given in Appendix D. ■

Although Lemma 1 suggests to choose an all-one vector for a row of \mathbf{B}_{eff} , choosing all-one vectors for multiple rows of \mathbf{B}_{eff} can aid the master node to average the corresponding error-locator polynomials thereby reducing the error rate of localization. Therefore, the following proposition uses Proposition 2 and Lemma 1 to present a desired structure on \mathbf{B}_{eff} .

Proposition 4. *When σ_p^2 is small, a bound on the objective function in (21) can be maximized by (i) picking the all-one row as the first row of \mathbf{B}_{eff} , (ii) picking $v - 1$ ones at random positions with uniform distribution for the other rows.*

Proof: We refer the readers to the proof given in Appendix E. ■

The strategy proposed in Proposition 4 ensures that only one error locator polynomial out of M polynomials has the maximum degree v , whereas the rest of the $M - 1$ polynomials have degree $v - 1$. Since degree $v - 1$ polynomials can have $v - 1$ distinct locations of the $v - 1$ Byzantine workers, the master node, without exact information on the locations, cannot perform the averaging operation among them. We highlight that \mathbf{B}_{eff} obtained from Proposition 4 may not give us \mathbf{B}_{eff}^\dagger , however, it is an effective way to directly generate the base matrices without computational burden.

In the rest of this section, we propose two strategies using which the Byzantine workers can locally generate their base matrices, satisfying a global structure on \mathbf{B}_{eff} . In particular, since their colluding channels have limited capacity, the proposed variants are based on the strength of the colluding channels.

A. Strongly Colluding Attack

In this threat model, we assume that the Byzantine workers have access to a high-capacity colluding channel in order to jointly arrive at \mathbf{B}_{eff} . In particular, we assume that one of the Byzantine worker nodes, is a master Byzantine worker, which possesses the knowledge of all the underlying parameters of

ALCC. Subsequently, it chooses \mathbf{B}_{eff} appropriately (this could be a solution of Problem 4 or Proposition 4) and distributes it to the other Byzantine worker nodes. Finally, all the Byzantine workers design the entries of their noise matrices $\mathbf{E}_{i_1}, \mathbf{E}_{i_2}, \dots, \mathbf{E}_{i_v}$ according to the columns of \mathbf{B}_{eff} .

Definition 1. An attack model is referred to as a strongly colluding model when the Byzantine worker nodes explicitly communicate \mathbf{B}_{eff} in their colluding channel.

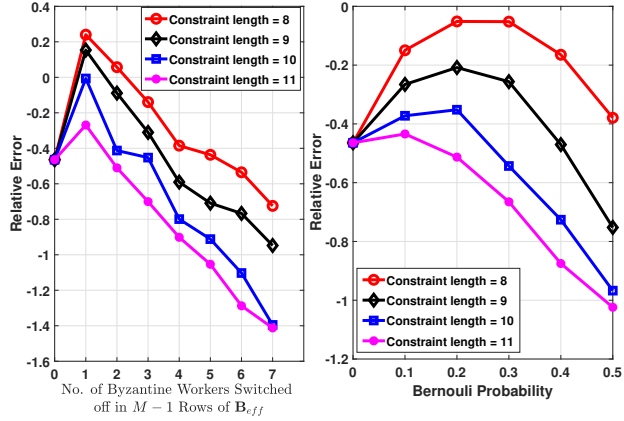


Fig. 6: Average relative error (in dB scale) of ALCC against strongly and weakly colluding attacks with parameters $N = 31, \tau = 0, K = 15, \beta = 1.5, k = 5, t = 3, \sigma = 10^6$. Here, the non-zero entries of noise matrices $\{\mathbf{E}_{i_a}\}$ are i.i.d. as $\mathcal{CN}(10, 10^2)$.

For the scenarios when the colluding channel between the Byzantine worker nodes cannot support high communication overhead, we propose an alternative model, wherein the master Byzantine worker broadcasts a *common seed*, enabling the other Byzantine workers to generate their column of \mathbf{B}_{eff} .

B. Weakly Colluding Attack

Unlike the strongly colluding attack, in this model, leveraging its knowledge of the ALCC parameters the master Byzantine worker selects a probability value $p \in (0, 1)$ instead of \mathbf{B}_{eff} . Subsequently, a suitably quantized version of p is broadcast to the other Byzantine workers, ensuring compatibility with communication constraints. Thereafter, each Byzantine worker constructs its column in \mathbf{B}_{eff} by generating its entries in a statistically independent manner using a Bernoulli process with probability p . Since identical p is used at all the Byzantine workers, this process is equivalent to generating $\mathbf{B}_{eff} \sim \text{Bernoulli}(p)$, where p denotes the probability associated with bit 0. While this threat model incurs less communication overhead over the strongly colluding model, it may not generate \mathbf{B}_{eff} with the structure of Proposition 4 at each instant, thus justifying its name.

Definition 2. An attack model is referred to as a weakly colluding model, when Byzantine workers communicate the value of p to locally generate their base matrices.

Proposition 5. When σ_p^2 is small, a reasonable strategy to pick p under the weakly colluding model is to solve

$$p^* = \arg \min_{p \in (0,1)} \frac{1}{Mv} \mathbb{E}[N_0] + \frac{1}{M} \mathbb{E}[N_1], \quad (22)$$

where N_0 denotes the number of zero entries in \mathbf{B}_{eff} and N_1 denotes the number of rows in \mathbf{B}_{eff} that have all ones.

Proof: We refer the readers to the proof given in Appendix F. ■

To showcase the impact of both the colluding attacks, we conduct experiments while computing the function $\mathbf{f}(\mathbf{X}) = \mathbf{X}^T \mathbf{X}$, such that $\mathbf{X} \in \mathbb{R}^{20 \times 5}$ in the presence of $v = 8$ Byzantine worker nodes at precision noise variance $\sigma_p^2 = 0.1$, while using joint localization with varying constraint lengths. For the strongly colluding case, the first row of \mathbf{B}_{eff} has all ones, whereas the other rows have variable number of ones. For weakly colluding case, we generate the rows of \mathbf{B}_{eff} using different probability values. The other parameters used for the experiments are $N = 31, \tau = 0, K = 15, \beta = 1.5, t = 3, \sigma = 10^6$. Here, the non-zero entries of noise matrices $\{\mathbf{E}_{i_a}\}$ are i.i.d. as $\mathcal{CN}(10, 10^2)$. We present these experimental results in Fig. 6. The plots confirm that the Byzantine worker nodes can use the results of Proposition 4 and Proposition 5 to effectively design their base matrices when $\sigma_p^2 > 0$. Further, under the weakly colluding attack model, we obtain p^* using the closed form expression. For instance, for our experiments, with $v = \lfloor \frac{N-K}{2} \rfloor = 8$, we obtain $p^* = 0.257$. As illustrated in Fig. 6, the worst-case accuracy for constraint length 8 occurs around this probability value, confirming that our theoretically derived p^* closely matches the empirical observation. From the viewpoint of the master node, the plots indicate that the only way to alleviate the impact of the proposed attacks is to increase the computational complexity, which may not be desirable. Overall, the plots in Fig. 6 confirm that in contrary to the approach of injecting noise on every component of their computations, the Byzantine worker nodes must carefully modify their base matrices when $\sigma_p^2 > 0$.

VII. SUMMARY

We have addressed an open problem raised by [18] and have identified how the nature of the computations returned by Byzantine worker nodes in ALCC allows the use of error correction algorithms from DFT codes. We have showed that our framework provides significantly higher accuracy than that of [18] in the presence of Byzantine worker nodes. Moreover, we have demonstrated that when the variance of the precision noise is negligible and when the number of Byzantine workers is small, our scheme achieves accuracy numbers close to that of the ALCC scheme without Byzantine worker nodes. We also discussed

a variant of ALCC comprising both reliable and unreliable worker nodes. For this setting, we proposed a customized strategy for assigning evaluations to the unreliable worker nodes which further reduces the overall relative error of ALCC framework. As the final contribution of this work, we studied the vulnerabilities of secure ALCC against colluding attacks from the Byzantine worker nodes. Subsequently, we proposed two colluding attacks, which suggest a new sparsity structure on the noise matrices in contrast to the presumption that noise matrices should be fully non-zero.

REFERENCES

- [1] V. K. Garg, *Elements of distributed computing*, in John Wiley and Sons, 2002.
- [2] J. R. Douceur, “The sybil attack,” in *International workshop on peer-to-peer systems*, Berlin, Heidelberg: Springer Berlin Heidelberg, 2002.
- [3] M. Satyanarayanan, “Integrating security in a large distributed system,” in *ACM Trans. Comput. Syst.*, vol. 7, no. 3, pp. 247-280, Aug. 1989.
- [4] Yaron Minsky, Robbert van Renesse, Fred B. Schneider, and Scott D. Stoller, “Cryptographic support for fault-tolerant distributed computing,” in proceedings of the *7th workshop on ACM SIGOPS European workshop: Systems support for worldwide applications (EW 7)*, New York, NY, USA, pp. 109–114, 1996.
- [5] Q. Yu, M. A. Maddah-Ali and A. S. Avestimehr, “Straggler mitigation in distributed matrix multiplication: Fundamental limits and optimal coding,” in *IEEE Transactions on Information Theory*, vol. 66, no. 3, pp. 1920-1933, March 2020.
- [6] H. Yang and J. Lee, “Secure distributed computing with straggling servers using polynomial codes,” in *IEEE Transactions on Information Forensics and Security*, vol. 14, no. 1, pp. 141-150, Jan. 2019.
- [7] Q. Yu and A. S. Avestimehr, “Coded computing for resilient, secure, and privacy-preserving distributed matrix multiplication,” in *IEEE Transactions on Communications*, vol. 69, no. 1, pp. 59-72, Jan. 2021
- [8] R. G. L. D’Oliveira, S. El Rouayheb and D. Karpuk, “GASP codes for secure distributed matrix multiplication,” in *IEEE Transactions on Information Theory*, vol. 66, no. 7, pp. 4038-4050, July 2020.
- [9] Q. Yu and A. S. Avestimehr, “Entangled polynomial codes for secure, private, and batch distributed matrix multiplication: breaking the cubic barrier,” *IEEE ISIT*, 2020.
- [10] Soleymani et al. “List-decodable coded computing: Breaking the adversarial toleration barrier,” *IEEE Journal on Selected Areas in Information Theory*, vol. 2, no. 3, pp. 867-878, 2021.
- [11] C. S. Yang and A. S. Avestimehr, “Coded computing for secure Boolean computations,” in *IEEE Journal on Selected Areas in Information Theory*, vol. 2, no. 1, pp. 326-337, March 2021.
- [12] Yang et al., “Secure coded computation for efficient distributed learning in mobile IoT,” in *2021 18th Annual IEEE SECON*, 2021.
- [13] M. Kim and J. Lee, “Private secure coded computation,” in *IEEE ISIT*, Paris, France, 2019, pp. 1097-1101.
- [14] A. Shamir, “How to share a secret,” *Communications of the ACM*, vol. 22, no. 11, pp. 612–613, 1979.
- [15] M. Soleymani, H. Mahdavifar and A. S. Avestimehr, “Analog privacy-preserving coded computing,” in *IEEE International Symposium on Information Theory*, Melbourne, Australia, 2021, pp. 1865-1870.
- [16] Mahdi Soleymani, Hessam Mahdavifar, A. Salman Avestimehr, “Privacy-preserving distributed learning in the analog domain,” in *arXiv preprint arXiv:2007.08803*, 2020.
- [17] Q. Yu, S. Li, N. Raviv, S. M. M. Kalan, M. Soltanolkotabi, and S. A. Avestimehr, “Lagrange coded computing: Optimal design for resiliency, security, and privacy,” in *22nd Int. Conf. Artif. Intell. Stat.*, pp. 1215-1225, 2019.
- [18] M. Soleymani, H. Mahdavifar and A. S. Avestimehr, “Analog Lagrange coded computing,” in *IEEE Journal on Selected Areas in Information Theory*, vol. 2, no. 1, pp. 283-295, March 2021.

[19] Petitcolas, Fabien AP. "Kerckhoffs' principle," *Encyclopedia of Cryptography, Security and Privacy*, Cham: Springer Nature Switzerland, pp. 1342-1343, 2025.

[20] Leslie Lamport, Robert Shostak, and Marshall Pease, "The Byzantine generals problem," in *ACM Trans. Program. Lang. Syst.*, vol. 4, no. 3, pp. 382-401, July 1982.

[21] T. G. Marshall, "Coding of real-number sequences for error correction: A digital signal processing problem," in *IEEE JSAC*, vol. 2, no. 2, pp. 381-392, March 1984.

[22] G. Rath and C. Guillemot, "Subspace-based error and erasure correction with DFT codes for wireless channels," in *IEEE Transactions on Signal Processing*, vol. 52, no. 11, pp. 3241-3252, Nov. 2004.

[23] G. Takos and C. N. Hadjicostis, "Determination of the number of errors in DFT codes subject to low-level quantization noise," in *IEEE Transactions on Signal Processing*, vol. 56, pp. 1043-1054, March 2008.

[24] M. Vaezi and F. Labeau, "Generalized and extended subspace algorithms for error correction with quantized DFT codes," in *IEEE Trans. on Communications*, vol. 62, no. 2, pp. 410-422, February 2014.

[25] G. Rath and C. Guillemot, "ESPRIT-like error localization algorithm for a class of real number codes," in *IEEE Global Telecommunications Conference*, San Francisco, CA, USA, 2003, pp. 2203-2207.

[26] M. Vaezi and F. Labeau, "Least squares solution for error correction on the real field using quantized DFT codes," in *20th European Signal Processing Conference (EUSIPCO)*, Bucharest, Romania, 2012, pp. 2561-2565.

[27] S. Gupta and J. Harshan, "Analog Lagrange coded computing: On the curious case of adversarial workers," in *2024 National Conference on Communications (NCC)*, Chennai, India, 2024.

[28] R. Borah and J. Harshan, "On securing analog Lagrange coded computing from colluding adversaries," in *2024 IEEE International Symposium on Information Theory (ISIT)*, Athens, Greece, 2024.

[29] M. Fahim and V. R. Cadambe, "Numerically Stable Polynomially Coded Computing," in *IEEE Transactions on Information Theory*, vol. 67, no. 5, pp. 2758-2785, May 2021.

[30] A. Ramamoorthy and L. Tang, "Numerically Stable Coded Matrix Computations via Circulant and Rotation Matrix Embeddings," in *IEEE Transactions on Information Theory*, vol. 68, no. 4, pp. 2684-2703, April 2022.

[31] H. P. Liu, M. Soleymani and H. Mahdavifar, "Differentially Private Coded Computing," in *IEEE International Symposium on Information Theory (ISIT)*, Taipei, Taiwan, 2023.

[32] X. Martínez-Luaña, M. Fernández-Veiga and R. P. Díaz-Redondo, "Privacy-aware Berrut Approximated Coded Computing applied to Federated Learning," in *IEEE International Workshop on Information Forensics and Security (WIFS)*, Rome, Italy, 2024.

[33] J. So, B. Güler and A. S. Avestimehr, "CodedPrivateML: A Fast and Privacy-Preserving Framework for Distributed Machine Learning," in *IEEE Journal on Selected Areas in Information Theory*, vol. 2, no. 1, pp. 441-451, March 2021.

[34] A. B. Das and A. Ramamoorthy, "Coded Sparse Matrix Computation Schemes That Leverage Partial Stragglers," in *IEEE Transactions on Information Theory*, vol. 68, no. 6, pp. 4156-4181, June 2022.

[35] T. Jahani-Nezhad and M. A. Maddah-Ali, "Berrut Approximated Coded Computing: Straggler Resistance Beyond Polynomial Computing," in *IEEE Transactions on Pattern Analysis and Machine Intelligence*, vol. 45, no. 1, pp. 111-122, 1 Jan. 2023.

[36] Moradi, Parsa, Behrooz Tahmasebi, and Mohammad Maddah-Ali. "Coded computing for resilient distributed computing: A learning-theoretic framework." in *Advances in Neural Information Processing Systems*, 2024.

[37] S. Hong, H. Yang, Y. Yoon and J. Lee, "Group-Wise Verifiable Coded Computing Under Byzantine Attacks and Stragglers," in *IEEE Transactions on Information Forensics and Security*, vol. 19, pp. 4344-4357, 2024.

[38] A. B. Das and A. Ramamoorthy, "A Unified Treatment of Partial Stragglers and Sparse Matrices in Coded Matrix Computation," in *IEEE Journal on Selected Areas in Information Theory*, vol. 3, no. 2, pp. 241-256, June 2022.

APPENDIX

A. Proof of Proposition 1

For each pair $\bar{u} \in [u], \bar{h} \in [h]$, let $\mathbf{r}_{\bar{u}\bar{h}} = [\mathbf{R}_1(\bar{u}, \bar{h}) \ \mathbf{R}_2(\bar{u}, \bar{h}) \ \dots \ \mathbf{R}_N(\bar{u}, \bar{h})]$ corresponds to a vector carved from the (\bar{u}, \bar{h}) -th entry of each \mathbf{R}_i . In total, the master node receives $M = \bar{u} \times \bar{h}$ such vectors from the worker nodes as depicted in the following matrix $\mathbf{R}_{eff} \in \mathbb{R}^{M \times N}$, where each row captures a received vector $\mathbf{r}_{\bar{u}\bar{h}}$ of length N .

$$\mathbf{R}_{eff} = \begin{bmatrix} \mathbf{R}_1(1, 1) & \mathbf{R}_2(1, 1) & \dots & \mathbf{R}_N(1, 1) \\ \mathbf{R}_1(1, 2) & \mathbf{R}_2(1, 2) & \dots & \mathbf{R}_N(1, 2) \\ \vdots & \vdots & \vdots & \vdots \\ \mathbf{R}_1(1, h) & \mathbf{R}_2(1, h) & \dots & \mathbf{R}_N(1, h) \\ \mathbf{R}_1(2, 1) & \mathbf{R}_2(2, 1) & \dots & \mathbf{R}_N(2, 1) \\ \vdots & \vdots & \vdots & \vdots \\ \mathbf{R}_1(u, h) & \mathbf{R}_2(u, h) & \dots & \mathbf{R}_N(u, h) \end{bmatrix}.$$

Note that, when $A = 0$, the set of vectors $\{\mathbf{r}_{\bar{u}\bar{h}}\}$ represents codewords from a K -dimensional Discrete Fourier Transform (DFT) code with blocklength N . To justify this claim, recall the encoding stage of ALCC, where the encoded matrix polynomial $l(z) \in \mathbb{R}^{m \times n}[z]$ is evaluated at the N -th roots of unity to distribute the set of evaluations $\{u(l_i) \in \mathbb{R}^{m \times n} \mid i \in [N]\}$ among N worker nodes. Subsequently, each worker node computes the target function $f : \mathbb{R}^{m \times n} \rightarrow \mathbb{R}^{u \times h}$, and returns the result $f(u(l_i)) \in \mathbb{R}^{u \times h}$ to the master node. Since the target function $f(\cdot)$ is a polynomial of degree D , applying it on each share $u(l_i) \in \mathbb{R}^{m \times n}$, results in a polynomial evaluation $f(u(l_i)) \in \mathbb{R}^{u \times h}$ of the matrix polynomial $f(l(z)) \in \mathbb{R}^{u \times h}$, where the effective degree of $f(l(z))$ is $\tilde{D} = (k + t - 1)D$. Let $\mathbf{m}_{\bar{u}\bar{h}}$ represent a row vector of length $K = \tilde{D} + 1$ containing the coefficients of the scalar polynomial corresponding to the (\bar{u}, \bar{h}) -th entry of the matrix polynomial $f(l(z))$. Then, the set of vectors $\mathbf{r}_{\bar{u}\bar{h}}$ received during the reconstruction stage of ALCC can be represented as $\mathbf{r}_{\bar{u}\bar{h}} = \mathbf{m}_{\bar{u}\bar{h}} \mathbf{G}$, for each $\bar{u} \in [u], \bar{h} \in [h]$, where the matrix \mathbf{G} is represented as

$$\mathbf{G} = \begin{bmatrix} 1 & 1 & 1 & \dots & 1 \\ 1 & \omega_N^1 & \omega_N^2 & \dots & \omega_N^{(N-1)} \\ 1 & \omega_N^2 & \omega_N^4 & \dots & \omega_N^{2(N-1)} \\ \vdots & \vdots & \vdots & \ddots & \vdots \\ 1 & \omega_N^{(K-1)} & \omega_N^{2(K-1)} & \dots & \omega_N^{(K-1)(K-1)} \end{bmatrix}_{K \times N}, \quad (23)$$

and $\omega_N = e^{-2\pi i/N}$ is the N -th root of unity. Note that, the above matrix \mathbf{G} is identical to the matrix generated by taking the first K rows from the DFT matrix \mathbf{W}_N of order N whose (m, n) -th element is

represented as $\mathbf{W}_N(m, n) = \frac{1}{\sqrt{N}} \omega_N^{(m-1)(n-1)}$, for $1 \leq m \leq N$ and $1 \leq n \leq N$. This results from the fact that the generator matrix of an (N, K) DFT code consists of any K rows from the DFT matrix of order N [21]. Therefore, in the absence of Byzantine worker nodes, the set of vectors, $\{\mathbf{r}_{\bar{u}\bar{h}} \mid \bar{u} \in [u], \bar{h} \in [h]\}$ represents the codewords of an (N, K) DFT code. Furthermore, in the presence of A Byzantine worker nodes, where $0 < A < N$, the vector $\mathbf{r}_{\bar{u}\bar{h}}$ at the decoder of ALCC represents a noisy codeword of (N, K) DFT code. Since, (N, K) DFT codes have error-correction capability of at most $\lfloor \frac{N-K}{2} \rfloor$ errors, their corresponding error-correction algorithms can be applied on each noisy codeword $\mathbf{r}_{\bar{u}\bar{h}}$ as long as $A \leq \lfloor \frac{N-K}{2} \rfloor$. Finally, since the error vectors are real-valued, infinite precision on floating-point representation is necessary to perfectly localize and cancel these errors. This completes the proof.

B. Proof of Theorem 1

Recall that $\bar{g}(z)$ denotes error-locator polynomial of degree A , given by $\bar{g}(z) = g(z) + e(z)$. In particular, we write $g(z) = g_0 + g_1 z + \dots + g_A z^A$ and $e(z) = e_0 + e_1 z + \dots + e_A z^A$, where $\{g_0, g_1, \dots, g_A\}$ are the fixed coefficients of the error-locator polynomial, and $\{e_0, e_1, \dots, e_A\}$ are the coefficients of $e(z)$, each distributed as $\mathcal{CN}(0, \sigma_p^2)$.

In the context of the theorem, let X_{i_a} be a root of $g(z)$ and X_{j_b} be another N -th root of unity such that $X_{i_a} \neq X_{j_b}$ and $g_{\bar{u}\bar{h}}(z)|_{z=X_{i_a}} \neq 0$. During the process of recovering the location of the errors, X_{j_b} is incorrectly decoded as the root of $\bar{g}(z)$ if $\|\bar{g}(X_{j_b})\|^2 < \|\bar{g}(X_{i_a})\|^2$. Therefore, to characterize this error event, we define $\|\bar{g}(X_{i_a})\|^2$ and $\|\bar{g}(X_{j_b})\|^2$ as two random variables and write

$$PEP_{j_b, i_a} = \text{Prob}(\|c + \bar{e}\|^2 \leq \|e\|^2), \quad (24)$$

where $c = g(z)|_{z=X_{j_b}}$, $\bar{e} = e(z)|_{z=X_{j_b}}$ and $e = e(z)|_{z=X_{i_a}}$. Expressing $X_{j_b} = e^{i\theta_b}$ such that $\theta_b = \frac{2\pi j_b}{N}$, and $X_{i_a} = e^{i\theta_a}$ such that $\theta_a = \frac{2\pi i_a}{N}$, the variables \bar{e} and e in (24) can be expanded as $\bar{e} = e_0 + E_{\theta_b}$, $e = e_0 + E_{\theta_a}$, where

$$E_{\theta_b} = e_1(e^{i\theta_b}) + e_2(e^{i2\theta_b}) + \dots + e_A(e^{iA\theta_b}), \quad (25)$$

and

$$E_{\theta_a} = e_1(e^{i\theta_a}) + e_2(e^{i2\theta_a}) + \dots + e_A(e^{iA\theta_a}). \quad (26)$$

After algebraic manipulation, we can rewrite (24) as,

$$PEP_{j_b, i_a} = \text{Prob}(\|c + e_0 + E_{\theta_b}\|^2 \leq \|e_0 + E_{\theta_a}\|^2). \quad (27)$$

Although (27) has $A + 1$ complex random variables, we further reduce it to A complex variables by marginalizing (27) over the random variable e_0 . Continuing from (27), we write all the complex variables in terms of their in-phase and quadrature components as $c = c_I + \iota c_Q$, $E_{\theta_b} = y_I + \iota y_Q$, $E_{\theta_a} = z_I + \iota z_Q$, and $e_0 = e_I + \iota e_Q$. Further, the condition $\|c + e_0 + E_{\theta_b}\|^2 \leq \|e_0 + E_{\theta_a}\|^2$ can be rewritten as,

$$(c_I + y_I + e_I)^2 + (c_Q + y_Q + e_Q)^2 \leq (e_I + z_I)^2 + (e_Q + z_Q)^2,$$

which can further be simplified into

$$2e_I(c_I + y_I - z_I) + 2e_Q(c_Q + y_Q - z_Q) \leq z_I^2 + z_Q^2 - (c_I + y_I)^2 - (c_Q + y_Q)^2.$$

Fixing the random variables, y_I, y_Q, z_I, z_Q to specific realizations, the scalar $2e_I(c_I + y_I - z_I) + 2e_Q(c_Q + y_Q - z_Q)$ is a Gaussian random variable with zero mean and variance $2\sigma_p^2[(c_I + y_I - z_I)^2 + (c_Q + y_Q - z_Q)^2]$. Using r to denote the above random variable, the pairwise probability of error expression conditioned on y_I, y_Q, z_I, z_Q can be written as,

$$\text{Prob}(r \leq z_I^2 + z_Q^2 - (c_I + y_I)^2 - (c_Q + y_Q)^2),$$

which can also be lower bounded as

$$\text{Prob}(r \leq -(c_I + y_I)^2 - (c_Q + y_Q)^2).$$

The above lower bound is valid since $z_I^2 + z_Q^2$ is always non-negative. Further, since r is zero mean, we rewrite the above as

$$\text{Prob}(r \geq (c_I + y_I)^2 + (c_Q + y_Q)^2).$$

Using the standard definition of Q-function, we write the above expression as,

$$Q\left(\frac{(c_I + y_I)^2 + (c_Q + y_Q)^2}{\sqrt{2\sigma_p^2((c_I + y_I - z_I)^2 + (c_Q + y_Q - z_Q)^2)}}\right),$$

by using the variance of the random variable r . Subsequently, using the Chernoff bound approximation, the above expression can be written as,

$$e^{-\frac{((c_I + y_I)^2 + (c_Q + y_Q)^2)^2}{4\sigma_p^2((c_I + y_I - z_I)^2 + (c_Q + y_Q - z_Q)^2)}}. \quad (28)$$

Finally, when taking expectation over the underlying random variables e_1, e_2, \dots, e_A , we get a lower bound

on (28) as

$$\mathbb{E}_{\{e_1, e_2, \dots, e_A\}} \left\{ e^{-\frac{((c_I + y_I)^2 + (c_Q + y_Q)^2)^2}{4\sigma_p^2((c_I + y_I - z_I)^2 + (c_Q + y_Q - z_Q)^2)}} \right\}. \quad (29)$$

In the rest of the proof, we provide a lower bound on (29).

In (28), note that y_I and y_Q are independent Gaussian random variables with zero mean and variance $\frac{A\sigma_p^2}{2}$. This follows from (25). Similarly, $y_I - z_I$ and $y_Q - z_Q$ are also independent Gaussian random variables with mean zero and variance

$$\sigma_{diff}^2 = \sigma_p^2(A - (\cos(\theta_d) + \cos(2\theta_d) + \dots + \cos(A\theta_d))), \quad (30)$$

such that $\theta_d = \theta_a - \theta_b$. When σ_p^2 is much smaller compared to the constants c_I and c_Q , then we observe that we can choose a positive constant η such that

$$\frac{\eta((c_I + y_I - z_I)^2 + (c_Q + y_Q - z_Q)^2)}{((c_I + y_I)^2 + (c_Q + y_Q)^2)} > 1,$$

with a probability close to one. Therefore, we can get a lower bound on PEP_{j_b, i_a} as,

$$\geq \mathbb{E}_{\{e_1, e_2, \dots, e_A\}} \left\{ e^{-\frac{\eta((c_I + y_I - z_I)^2 + (c_Q + y_Q - z_Q)^2)}{4\sigma_p^2}} \right\}. \quad (31)$$

Given that $y_I - z_I$ and $y_Q - z_Q$ are statistically independent, (31) can be rewritten as

$$PEP_{j_b, i_a} \geq \mathbb{E}_{(y_I - z_I)} \left\{ e^{-\frac{\eta(c_I + y_I - z_I)^2}{4\sigma_p^2}} \right\} \times \mathbb{E}_{(y_Q - z_Q)} \left\{ e^{-\frac{\eta(c_Q + y_Q - z_Q)^2}{4\sigma_p^2}} \right\}. \quad (32)$$

For each of the above two terms, we note that closed-form expressions can be computed to respectively obtain

$$\mathbb{E}_{(y_I - z_I)} \left\{ e^{-\frac{(c_I + y_I - z_I)^2}{4\sigma_p^2}} \right\} = \frac{\sqrt{2}\sigma_p}{\sqrt{\sigma_{diff}^2}\sqrt{\eta + \gamma}} e^{-\frac{\eta c_I^2 \gamma}{4\sigma_p^2(\eta + \gamma)}}, \quad (33)$$

and

$$\mathbb{E}_{(y_Q - z_Q)} \left\{ e^{-\frac{(c_Q + y_Q - z_Q)^2}{4\sigma_p^2}} \right\} = \frac{\sqrt{2}\sigma_p}{\sqrt{\sigma_{diff}^2}\sqrt{\eta + \gamma}} e^{-\frac{\eta c_Q^2 \gamma}{4\sigma_p^2(\eta + \gamma)}}, \quad (34)$$

where σ_{diff}^2 is as given in (30) and $\gamma = \frac{2\sigma_p^2}{\sigma_{diff}^2}$. Finally, substituting the above expressions in (32), we get

$$PEP_{j_b, i_a} \geq PL_{j_b, i_a} \triangleq \frac{\kappa}{(1 + \kappa)} e^{-\frac{\eta(c_I^2 + c_Q^2)\kappa}{4\sigma_p^2(1 + \kappa)}}, \quad (35)$$

where η, c_I, c_Q are constants which depends on e and the indices j_b, i_a , and $\kappa = \frac{2}{\eta \sum_{l=1}^A 1 - \cos(l\theta_d)}$, where $\theta_d = \theta_a - \theta_b$. This completes the proof.

C. Proof of Proposition 2

When $\sigma_p^2 = 0$, i.e., when there is no precision noise errors, the choice of $\mathbf{B}_{ia} = \mathbf{J}_{u \times h}$ for every $a \in [v]$, where $v = \lfloor \frac{N-K}{2} \rfloor$, would imply that the uh error-locator polynomials recovered at the master node are identical. As a result, solving for the roots of one of the polynomials is sufficient to localize the errors. However, when $\sigma_p^2 > 0$, all the uh error-locator polynomials recovered at the master node are noisy versions of one polynomial, whose degree is v . Moreover, the noise component added on the coefficients of the polynomials are also statistically independent. As a consequence, we can average the coefficients of all the error locator polynomials and then solve for the roots. As the process of averaging reduces the effective precision noise variance of the coefficients, the lower bound on pairwise error probability reduces due to Corollary 1. As a result, the error rate of localization is expected to reduce for all $v(N-v)$ pairs defined in (9). With that, the end-to-end accuracy of ALCC also improves compared to the case when independent localization is performed in the DFT decoder. This completes the proof.

D. Proof of Lemma 1

In the expression on the lower bound in Theorem 1 (which is the expression for $PL_{(i_a^*, i_a^* + 1, c)}$), we note that,

$$\frac{\kappa}{1 + \kappa} = \frac{2}{2 + \eta \sum_{l=1}^{A_c} (1 - \cos(l\theta_d))},$$

where $\theta_d = \frac{2\pi}{N}(|i_a^* - (i_a^* + 1)|) = \frac{2\pi}{N}$. Since $(1 - \cos(l\theta_d))$ is a non-negative number for any $l \in [A_c]$ and N , the term $\sum_{l=1}^{A_c} (1 - \cos(l\frac{2\pi}{N}))$ is a non-decreasing function of A_c . Therefore, $\frac{\kappa}{1 + \kappa}$ is a non-increasing function of A_c . In addition, since $\frac{\kappa}{1 + \kappa}$ is in the exponent of $e^{-\frac{\eta(c_I^2 + c_Q^2)\kappa}{4\sigma_p^2(1 + \kappa)}}$, it is evident that the term $e^{-\frac{\eta(c_I^2 + c_Q^2)\kappa}{4\sigma_p^2(1 + \kappa)}}$ is a non-decreasing function of A_c . Overall, the lower bound is the product of the following three terms A_c , $\frac{\kappa}{1 + \kappa}$, $e^{-\{\frac{d\kappa}{\sigma_p^2(1 + \kappa)}\}}$, for some constant d , which are non-decreasing, non-increasing, and non-decreasing functions of A_c , respectively. To study the behavior of this function with respect to A_c , we apply \log_e on it to obtain $\log_e(A_c) + \log_e \frac{\kappa}{1 + \kappa} - \frac{d}{\sigma_p^2} \frac{\kappa}{1 + \kappa}$. Since $\log_e \frac{\kappa}{1 + \kappa}$ is sub-linear, the term $\frac{d}{\sigma_p^2} \frac{\kappa}{1 + \kappa} + \log_e(A_c)$ dominates the lower bound when σ_p^2 is small, and therefore, the lower bound increases as A_c increases from 1 to v . This completes the proof.

E. Proof of Proposition 4

From Proposition 2, \mathbf{B}_{eff}^\dagger should not be the all-one matrix. Also, from Lemma 1, each row of \mathbf{B}_{eff}^\dagger must contain as many ones as possible. This implies that the number of ones in every row must be either v or $v-1$. Let us suppose that out of the M rows, Ω rows of \mathbf{B}_{eff}^\dagger have all ones and the rest of the $M-\Omega$ rows have $v-1$ ones at some positions. Under this situation, we prove that the optimal choice of Ω is

one in order to maximize the objective function of Problem 4. With Ω rows of \mathbf{B}_{eff}^\dagger containing all-ones, the master node can average them to obtain one error-locator polynomial, and the rest of the polynomials are in-tact. We arrange the polynomials such that the first polynomial captures the averaged degree v polynomial, while the remaining are degree $v - 1$ polynomials. With a total of $1 + M - \Omega$ polynomials, the master node proceeds to perform independent localization. Error event in the localization step occurs when either one of the polynomials experience errors. Therefore, with $M - \Omega + 1$ total polynomials, the right-hand side of the expression in (21) denoted by PL , can be expressed as

$$PL = \frac{1}{M - \Omega + 1} (v \times PL_{(i_a^*, i_a^* + 1, 1)}) + \frac{1}{M - \Omega + 1} \left(\sum_{n=2}^{M - \Omega + 1} (v - 1) \times PL_{(i_a^*, i_a^* + 1, n)} \right), \quad (36)$$

where $PL_{(i_a^*, i_a^* + 1, 1)}$ and $PL_{(i_a^*, i_a^* + 1, n)}$ denote the lower bound on pairwise error probability of averaged degree v polynomial, and n -th degree $v - 1$ polynomials, for $n \in [2 : M - \Omega + 1]$. Subsequently, using the derived expressions on lower bound in Theorem 1, the expression in (36)(which is applicable for $\Omega \geq 1$), can be expressed as

$$PL = \frac{1}{M - \Omega + 1} \times v \times \left(\frac{\kappa_1}{(1 + \kappa_1)} e^{-\frac{\Omega \eta (c_{I_v}^2 + c_{Q_v}^2) \kappa_1}{4\sigma_p^2 (1 + \kappa_1)}} \right) + \left(\frac{1}{M - \Omega + 1} \right) \times (v - 1) \times \left(\sum_{n=1}^{M - \Omega} \frac{\kappa_2}{(1 + \kappa_2)} e^{-\frac{\eta (c_{I_n}^2 + c_{Q_n}^2) \kappa_2}{4\sigma_p^2 (1 + \kappa_2)}} \right), \quad (37)$$

where $\kappa_1 = \frac{2}{\eta \sum_{l=1}^v 1 - \cos(l\theta_d)}$ and $\kappa_2 = \frac{2}{\eta \sum_{l=1}^{v-1} 1 - \cos(l\theta_d)}$, such that $\theta_d = \frac{2\pi}{N}$, and $c_{I_v}^2 + c_{Q_v}^2$, $c_{I_n}^2 + c_{Q_n}^2$ are the constants depend on i_a^* for averaged degree v polynomial and n -th degree $v - 1$ polynomials. Notice the presence of Ω in the exponent of the first term of (37). To prove that $\Omega = 1$ is the optimal choice, we need to show that

$$PL|_{\Omega=1} > PL|_{\Omega>1}, \quad (38)$$

and

$$PL|_{\Omega=1} > PL|_{\Omega=0}. \quad (39)$$

Towards proving (38) and (39), we replace all the pairwise error terms in the summation of second term in (37) by the maximum of of all $M - \Omega$ pairwise error terms i.e., $\max_{1 \leq n \leq M - \Omega} \left(\frac{\kappa_2}{(1 + \kappa_2)} e^{-\frac{\eta (c_{I_n}^2 + c_{Q_n}^2) \kappa_2}{4\sigma_p^2 (1 + \kappa_2)}} \right)$. Therefore, instead of finding the optimal \mathbf{B}_{eff}^\dagger which maximizes (37), we find \mathbf{B}_{eff} which aim to maximize the following expression which is an approximation of (37) denoted as PL_{approx} given by

$$PL_{approx} = \frac{1}{M - \Omega + 1} \times v \times \left(\frac{\kappa_1}{(1 + \kappa_1)} e^{-\frac{\Omega \eta (c_{I_v}^2 + c_{Q_v}^2) \kappa_1}{4\sigma_p^2 (1 + \kappa_1)}} \right) + \frac{M - \Omega}{M - \Omega + 1} \times (v - 1) \times \left(\frac{\kappa_2}{(1 + \kappa_2)} e^{-\frac{\eta (c_{I_{v-1}}^2 + c_{Q_{v-1}}^2) \kappa_2}{4\sigma_p^2 (1 + \kappa_2)}} \right), \quad (40)$$

where the second term denotes the maximum pairwise error probability term among $M - \Omega$ pairwise error terms of degree $v - 1$ polynomials and $c_{I_{v-1}}^2 + c_{Q_{v-1}}^2$ in the exponent is a constant depends on the index i_a^* . Therefore, due to the approximation in (40), instead of proving (38) and (39), we now prove for

$$PL_{approx}|_{\Omega=1} > PL_{approx}|_{\Omega>1}, \quad (41)$$

$$PL_{approx}|_{\Omega=1} > PL_{approx}|_{\Omega=0}. \quad (42)$$

In this context, when $\Omega = 0$, the remaining polynomials are of degree $v - 1$. Therefore, we have

$$PL_{approx}|_{\Omega=0} = (v - 1) \times \left(\frac{\kappa_2}{(1 + \kappa_2)} e^{-\frac{\eta(c_{I_{v-1}}^2 + c_{Q_{v-1}}^2)^{\kappa_2}}{4\sigma_p^2(1 + \kappa_2)}} \right). \quad (43)$$

On the other hand, when $\Omega = 1$, we have

$$PL_{approx}|_{\Omega=1} = \frac{1}{M} \times v \times \left(\frac{\kappa_1}{(1 + \kappa_1)} e^{-\frac{\eta(c_{I_{v-1}}^2 + c_{Q_{v-1}}^2)^{\kappa_1}}{4\sigma_p^2(1 + \kappa_1)}} \right) + \frac{M-1}{M} \times (v - 1) \times \left(\frac{\kappa_2}{(1 + \kappa_2)} e^{-\frac{\eta(c_{I_{v-1}}^2 + c_{Q_{v-1}}^2)^{\kappa_2}}{4\sigma_p^2(1 + \kappa_2)}} \right). \quad (44)$$

The above expression can be written as

$$PL_{approx}|_{\Omega=1} = \frac{1}{M} \times v \times \left(\frac{\kappa_1}{(1 + \kappa_1)} e^{-\frac{\eta(c_{I_{v-1}}^2 + c_{Q_{v-1}}^2)^{\kappa_1}}{4\sigma_p^2(1 + \kappa_1)}} \right) + PL_{approx}|_{\Omega=0}. \quad (45)$$

Finally, in the above expression, since the coefficient of $\frac{1}{M}$ is more than that of $\frac{M-1}{M}$ when σ_p^2 is small (due to Lemma 1), we can conclude

$$PL_{approx}|_{\Omega=1} > PL_{approx}|_{\Omega=0}.$$

Towards proving (41), we need to prove that PL_{approx} in (40) decreases as Ω increases in the range $[M]$. We immediately notice that the second term of (37) is a decreasing function of Ω for a given N, v and σ_p^2 . However, the first term of (37) is such that $\frac{1}{M-\Omega+1}$ increases with Ω , whereas the exponent term decreases with Ω . Along the similar lines of the proof of Lemma 1, when σ_p^2 is small, the exponent term dominates the inverse linear term, and therefore, the first term of (40) decreases with Ω . This completes the proof for (41). Further, note that, because of using the approximation of original expression (37) in (40), the above strategy does not yield the optimal \mathbf{B}_{eff}^\dagger , rather provides a near optimal choice, denoted as \mathbf{B}_{eff} . This completes the proof that only one row of \mathbf{B}_{eff} must contain the all-one row, whereas the other rows must be filled with $v - 1$ ones. Finally, in order to keep the choice of \mathbf{B}_{eff} non-deterministic to the master node, the positions of ones on those rows that have $v - 1$ must be chosen at random with uniform distribution. Thus, without loss of generality, in the statement of Proposition 4, we recommend using the all-one row for the first row, and the rest of the rows to be filled with $v - 1$ rows. This completes

the proof.

F. Proof of Proposition 5

Due to Lemma 1, when σ_p^2 is small, the lower bound on error rate of localization of an error locator polynomial is an increasing function of A_c , where A_c denotes the degree of the error locator polynomial, which also captures the number of non-zero entries of a row of \mathbf{B}_{eff} . As a consequence, \mathbf{B}_{eff} must be such that the average number of zeros (captured by $\mathbb{E}[N_0] = Mvp$) in it should be minimized. Also due to Proposition 2, given that the master node can perform averaging of all the degree v polynomials, the average number of rows that have all ones in it, denoted by $\mathbb{E}[N_1] = M(1 - p)^v$, should be minimized. Thus, combining the two objectives, we propose p^* in (22), which can be obtained in closed form as

$$p^* = 1 - \left((v - 1) \sqrt{\frac{1}{v}} \right). \quad (46)$$

Therefore, p^* can be obtained for a given choice of $v = \lfloor \frac{N-K}{2} \rfloor$, using (46). Finally, this value of p^* can be used to generate \mathbf{B}_{eff} at the Byzantine worker nodes. This completes the proof.